The calcineurin regulator Sarah enables acute and chronic forms of homeostatic plasticity at the *Drosophila* neuromuscular junction

Noah S. Armstrong[1,2] and C. Andrew Frank[1,2, 3]

[1]Department of Anatomy and Cell Biology, University of Iowa Carver College of Medicine, Iowa City, IA, United States; [2]Interdisciplinary Graduate Program in Neuroscience, University of Iowa, Iowa City, IA, United States; [3]Iowa Neuroscience Institute, University of Iowa, Iowa City, IA

*** Correspondence:**

C. Andrew Frank

andy-frank@uiowa.edu

Keywords: *Drosophila melanogaster*, NMJ, neurotransmission, plasticity, synaptic homeostasis, synaptic dysfunction, calcineurin, *sarah* (*sra*)

Abstract

The ability of synapses to maintain physiological levels of evoked neurotransmission is essential for neuronal stability. A variety of perturbations can disrupt neurotransmission, but synapses often compensate for disruptions and work to stabilize activity levels, using forms of homeostatic synaptic plasticity. Presynaptic homeostatic potentiation (PHP) is one such mechanism that is expressed at the model *Drosophila melanogaster* larval neuromuscular junction (NMJ) synapse. In PHP, neurotransmitter release increases in response to challenges to the synapse, resulting in the maintenance of evoked neurotransmission. Prior work separated PHP into two temporal phases, acute and chronic. Those data suggested that cytoplasmic calcium signaling was important for a long-term maintenance of PHP. Here we used a combination of transgenic *Drosophila* RNA interference and overexpression lines, along with NMJ electrophysiology, synapse imaging, and pharmacology to test if regulators of the calcium/calmodulin-dependent protein phosphatase calcineurin are necessary for the normal expression of acute or chronic forms of PHP. We found that either pre- or postsynaptic dysregulation of a *Drosophila* gene regulating calcineurin, *sarah* (*sra*), blocks PHP. Examination of tissue-specific data showed that increases and decreases in *sra* expression are both detrimental to PHP. Additionally, the acute and chronic phases of PHP are functionally separable depending entirely upon which *sra* genetic manipulation is used. Surprisingly, concurrent pre- and postsynaptic *sra* knockdown or overexpression ameliorated PHP blocks revealed in single tissue experiments. Pharmacological inhibition of calcineurin corroborated this latter finding. Our results suggest that a discrete balance of calcineurin signaling is needed across multiple synapse tissue types and over different temporal phases to stabilize peripheral synaptic outputs.

INTRODUCTION

Normal synapse function permits a pre-determined physiological range of activity. Challenges to synapse function can force activity beyond setpoint limits. To maintain stability, synaptic and circuit level homeostatic mechanisms exist in vertebrates and invertebrates (Davis, 2006, Marder, 2012, Pozo and Goda, 2010, Frank, 2014). Defects in homeostatic plasticity can impair the preservation of neuronal activity and may be associated with neurological conditions that display synaptic instabilities including ataxia, migraine, schizophrenia, Alzheimer's disease and epilepsy (Andre et al., 2018, Dickman and Wondolowski, 2013, Wondolowski and Dickman, 2013, Bliss et al., 2014). Synaptic homeostasis has also been implicated as being necessary for the manifestation of normal sleep behavior (Tononi and Cirelli, 2006, Kikuma et al., 2019). For these diverse behaviors or neurological disorders, the relevant synaptic activities or synaptic functional challenges operate on varying timescales, from minutes (e.g., perturbations that induce migraine) to years (e.g., conditions like Alzheimer's Disease). Yet there are significant gaps in understanding of how neuronal stability is maintained, across neural tissue types and over broad timescales.

We can address some of these gaps using model synapses, like the *Drosophila melanogaster* neuromuscular junction (NMJ). The *Drosophila* NMJ is a well-studied synapse (Menon et al., 2013). It is suitable for combining approaches in genetics, development, and electrophysiology (Jan and Jan, 1976). For homeostatic synaptic plasticity, the NMJ has been key for mechanistic discovery (Frank et al., 2020). One well-characterized form of homeostatic plasticity is called presynaptic homeostatic potentiation (PHP). PHP is initiated when postsynaptic glutamate receptors are impaired, decreasing quantal size. The synapse detects this impairment, and a muscle-to-nerve signaling process drives increased presynaptic glutamate release. The prevailing model is that potentiated release happens after retrograde signaling triggers an increase in presynaptic calcium influx through Ca_V2 voltage-gated calcium channels (Frank et al., 2006, Frank et al., 2009, Müller and Davis, 2012, Wang et al., 2014, Younger et al., 2013). This increase in presynaptic calcium influx coincides with an increased readily releasable pool (RRP) of synaptic vesicles (Harris et al., 2015, Müller et al., 2015, Müller et al., 2012, Weyhersmüller et al., 2011). These modifications drive the ability of the motor neuron to deliver more glutamate to the cleft, offsetting the decreased quantal size.

Temporally, PHP is separable into two phases: acute induction and chronic maintenance. Acute induction occurs rapidly in minutes (Frank et al., 2006), while chronic maintenance occurs over an extended developmental time (Davis et al., 1998, DiAntonio et al., 1999, Petersen et al., 1997). Acute PHP can be induced and expressed by applying glutamate receptor inhibitors, like Philanthotoxin-433 (PhTx) (Frank et al., 2006) or GYKI-53655 (Nair et al., 2021). For chronic PHP expression, glutamate receptors can be homeostatically challenged genetically using a loss of function mutation in *GluRIIA*^{SP16} (Petersen et al., 1997), RNAi-mediated knockdown of *GluRIII* RNAi (Brusich et al., 2015), or a variety of other genetic manipulations that impair glutamate receptor expression throughout development (reviewed in (Frank, 2014)). Each of these manipulations results in decreased quantal size, offset by increased quantal content, resulting in normal levels of evoked excitation.

The acute and chronic phases of PHP share similar expression mechanisms (Goel et al., 2017, Böhme et al., 2019, Müller et al., 2012), but data from our lab demonstrates that these phases of PHP are separable, both genetically and pharmacologically (James et al., 2019). We previously reported that a signaling modality including Gq, *Plc21C* (*Drosophila* PLCβ homolog), IP_3 receptors, and ryanodine receptors were necessary for the maintenance, but not the acute induction of PHP (James et al., 2019). IP_3 receptors and ryanodine receptors have dual pre- and postsynaptic functions by mediating the release of intracellular calcium from intracellular calcium stores (Kadamur and Ross, 2013, Philip et al., 2010). However, it is unclear which calcium-dependent molecules must be activated or regulated via the release of calcium from intracellular stores to sustain homeostatic signaling.

Calcineurin is a well conserved Ca^{2+}/calmodulin-dependent protein phosphatase that is found in most mammalian tissues but is expressed at high levels in the brain, and it has been shown to regulate ion channel function and trafficking, apoptosis, gene regulation, receptor trafficking, neuronal plasticity, and immune processes (Rusnak and Mertz, 2000, Furman and Norris, 2014, Musson and Smit, 2011, Baumgärtel and Mansuy, 2012). Calcineurin is also regulated by a family of proteins known as regulators of calcineurin (RCAN1), which are the product of down syndrome critical region 1 (DSCR1) gene (Park et al., 2009, Harris et al., 2005). There is evidence that suggests that RCAN family members inhibit calcineurin activity (Kingsbury and Cunningham, 2000, Lee et al., 2003). The *Drosophila* gene *sarah* (*sra*; also

known as *nebula*) encodes the only known ortholog of DSCR1 in *Drosophila* (Chang et al., 2003). Sra/Nebula/DSCR1 (herein: Sra) has been shown to physically associate with the catalytic subunit of calcineurin (Takeo et al., 2006). Evidence suggests that Sra inhibits calcineurin as calcineurin activity has been shown to be approximately 40% higher in *sra* mutants in comparison to controls or heterozygous mutants (Chang et al., 2003). *sra* gene function has been shown to be required for mitochondrial function (Chang and Min, 2005), female meiosis and egg activation (Takeo et al., 2006, Horner et al., 2006, Takeo et al., 2012), sleep regulation (Nakai et al., 2011) and learning (Chang et al., 2003).

Here we report that both increases and decreases in *sra* gene expression – in either presynaptic neuron or postsynaptic muscle – result in PHP impairment. Using genetics, we again found that acute and chronic phases of PHP were functionally separable, as specific *sra* manipulations compromised either acute or chronic PHP.

We found that tissue-specific manipulations of *sra* resulted in strong blocks of PHP. But surprisingly, dual tissue manipulations did not. Concurrent pre- and postsynaptic *sra* knockdown or overexpression led to weaker (or no) blocks of PHP compared to single tissue impairments. Consistent with this latter finding, global pharmacological inhibition of calcineurin via FK506 increases homeostatic capabilities following a chronic PHP challenge.

Taken together, our data highlight a novel idea: individual proteins like Sra are present in multiple synaptic tissues; if those factors are manipulated in tissue-specific ways, there can be profound defects in overall synapse stability. For a gene like *sra*, that might mean that global losses of function escape the most severe phenotypes. In the case of calcineurin signaling at the NMJ, it appears the strongest phenotypes might occur when there is an imbalance of calcineurin regulation between neuron and muscle. Our data provide a new model for testing how individual molecules contribute to homeostatic synaptic plasticity from different synaptic tissues.

METHODS

Drosophila husbandry and stocks

Drosophila melanogaster fruit flies were raised on a standard cornmeal and molasses medium prepared according to the recipe from the Bloomington *Drosophila* Stock Center (BDSC, Bloomington, IN). *Drosophila* husbandry was performed according to standard practices (Greenspan, 2004). Larvae were raised at 25□C or 29□C in humidity and light controlled (12 h light: 12 h dark) Percival DR-36VL incubators (Geneva Scientific).

w^{1118} (Hazelrigg et al., 1984) was used as a non-transgenic wild type stock. The null $GluRIIA^{SP16}$ mutant generated previously (Petersen et al., 1997). The *UAS-GluRIII* RNAi line that was used has been described previously (Brusich et al., 2015). GAL4 drivers that were used included the neuronal drivers *elaV*(*C155*)-*GAL4* (Lin and Goodman, 1994) and *Sca-GAL4* (Budnik et al., 1996) and the postsynaptic driver *BG57-GAL4* (Budnik et al., 1996). The *sra* RNAi line that used was *TRiP.JF02557* (BDSC:27260) and the *sra* overexpression line that was used was $sra^{EY07182}$ (BDSC:15991).

Electrophysiology and pharmacology

Wandering third instar larvae were collected and dissected for NMJ analysis. Both control and experimental conditions were performed in parallel using identical conditions. Dissections and recordings were performed in a modified HL3 saline (70 mM NaCl, 5 mM KCl, 5mM HEPES, 10 mM $NaHCO_3$, 115 mM sucrose, 4.2 mM trehalose, 0.5 mM $CaCl_2$ (unless otherwise noted), 10 mM $MgCl_2$, pH 7.2 (Stewart et al., 1994). Neuromuscular junction sharp electrode recordings were performed on muscles 6/7 of abdominal segments A2, A3, and A4. Miniature excitatory postsynaptic potentials (mEPSPs) and excitatory postsynaptic potentials (EPSPs) were conducted as previously described (Brusich et al., 2015, Spring et al., 2016, Yeates et al., 2017, James et al., 2019, Mallik and Frank, 2022).

Uncorrected quantal content was calculated per NMJ by dividing the average EPSP by the average mEPSP. Recordings were performed on a Leica microscope using a 10x objective and acquired using an Axoclamp 900A amplifier, Digidata 1440A acquisition system and pClamp10.7 (Molecular Devices) software. Data were analyzed using MiniAnalysis (Synaptosoft) and the Clampfit (Molecular Devices) programs. To generate mEPSP and EPSP traces for figures, (x,y) coordinates were pulled from the Clampfit program and imported into

GraphPad Prism (GraphPad) software. All traces display the recording that was at or closest to the calculated average of each specific condition.

Pharmacological agents were bath applied in recording saline at the final concentrations indicated in the text and figures. The agents included Philanthotoxin-433 (PhTx, Sigma-Aldrich), Cyclosporin A (Sigma-Aldrich), and FK506 (InvivoGen).

Immunostaining and analyses

Wandering third instar larvae were dissected on a sylgard Petri plate in HL3 and fixed using Bouin's fixative for 10 min. Larvae were washed with PBS containing 0.2% Triton X-100 (PBST) for 40 min, blocked for an hour with 2.5% BSA, and incubated overnight with primary antibodies at 4□C. This was followed with another 40 min of washes, and incubation in secondary antibodies for 1.5 hr at room temperature. The primary antibodies used were mouse anti-Synapsin (anti-Syn; 3C11) 1:50 (Developmental Studies Hybridoma Bank, Iowa City, IA) and rabbit anti-Dlg 1:15,000 (Budnik et al., 1996). The following fluorophore conjugated secondary were also used (Jackson ImmunoResearch Laboratories): goat anti-mouse 488 1:1000 (DyLight) and goat anti–rabbit 549 1:2000 (DyLight). Larval preparations were mounted in Vectashield (Vector Laboratories) and imaged at room temperature with a 700 Carl Zeiss laser scanning confocal microscope equipped with 63 × /1.4 NA oil immersion objective using separate channels with four laser lines (405, 488, 555, and 639 nm). Images were prepared for publication using Adobe Illustrator. Anti-Dlg boutons were counted in muscle after verifying that there was a corresponding cluster of anti-Syn staining in motor neurons.

Statistical analyses

Statistical significance was tested using either a Student's T-Test to compare one experimental data set directly to a control data set or using a one-way ANOVA with a Tukey's post-hoc test if multiple data sets were being compared. Specific p-value ranges used were as follows: *$p<0.05$, **$p<0.01$, and ***$p<0.001$. All statistical analyses were conducted using GraphPad Prism

software. Data were plotted in GraphPad Prism and final figures were compiled using Adobe Illustrator.

RESULTS

Concurrent neuron and muscle *sra* knockdown do not block PHP

PHP is most commonly assessed at the *Drosophila* NMJ using acute Philanthotoxin-433 (PhTx) application to test the rapid induction of PHP (Frank et al., 2006) or $GluRIIA^{SP16}$, the genetic null mutation used to test the chronic maintenance of PHP (Petersen et al., 1997). Both manipulations result in decreased mEPSP amplitude while quantal content increases as PHP mechanisms work to sustain evoked potentials near normal levels.

Given our prior data suggesting that dysregulation of calcium stores disrupted the maintenance of PHP (Brusich et al., 2015, James et al., 2019), we wanted to test whether combined pre- and postsynaptic *sra* loss-of-function conditions impaired PHP. To do this, we used a *Drosophila* line that contains both neuron and muscle GAL4 drivers to knockdown *sra* using RNAi and applied 20µM PhTx to test PHP induction. PhTx application decreased mEPSP amplitude for both driver control and *sra RNAi* conditions (**Figure 1A**) (Frank et al., 2006). Evoked potentials were maintained for the driver control (**Figure 1B**) because of the compensatory significant increase in quantal content (**Figure 1C**). Dual tissue knockdown of *sra* resulted in a mild decrease in evoked potentials following PhTx incubation. This might be consistent with a small defect in homeostatic plasticity, but there was still a significant increase in quantal content compared to non-drugged controls (**Figure 1A-D** and **Supplementary Table 1**). At a minimum, this indicated partially intact PHP induction and expression.

To test the maintenance of PHP, we used a *Drosophila* line that contains both neuron and muscle GAL4 drivers, along with *UAS-GluRIII RNAi* to provide a chronic homeostatic challenge (Brusich et al., 2015). Again, while there were significant decreases in evoked amplitude in *sra RNAi* synapses challenged with either PhTx or *GluRIII RNAi*, there were still compensatory increases in quantal content (Figure 1A-D). Our interpretation of these data is that PHP mechanisms are partially (or largely) intact when *sra* function is knocked down.

Concurrent neuron and muscle *sra* overexpression do not block PHP

We also acquired reagents to test if simultaneous pre- and postsynaptic overexpression of *sra* resulted in acute or chronic PHP impairment. We used the $sra^{EY07182}$ allele. This is a 5' P-element insertion allele in the endogenous *sra* locus with UAS binding sites for GAL4 transcriptional control upstream of the *sra* gene; this allows for conditional tissue specific overexpression of *sra*. Overexpression of *sra* neuronally using the pan neuronal driver, *elaV*, and $sra^{EY07182}$ has been shown to result in transcript levels that were approximately twofold higher than controls (Chang et al., 2003, Shaw and Chang, 2013, Lee et al., 2016).

For our electrophysiological experiments, there was a decrease in the EPSPs of muscle GAL4 >> $sra^{EY07182}$ ("*sra* OE" - overexpression) + *GluRIII RNAi* synapses compared to muscle GAL4 >> $sra^{EY07182}$ alone, but there was also a significant increase in quantal content (**Figure 1E-H** and **Supplementary Table 1**). Our interpretation of those data is that chronic PHP is partially (or mostly) intact.

Additionally, we there was no significant difference in the EPSPs of muscle GAL4 >> $sra^{EY07182}$ overexpression animals alone or genetically identical overexpression animals challenged with PhTx. This is because of increased presynaptic quantal content (**Figure 1E-H**). Taken as a whole, concurrent overexpression of *sra* both pre-and postsynaptically does not preclude homeostatic increases in quantal content. If anything, phenotypes are subtle, indicating partial impairments of PHP.

Postsynaptic *sra* knockdown impairs the induction of PHP but not its maintenance

While testing for dual-tissue functions for *sra* in PHP, we also conducted single-tissue experiments. First, we used the *UAS-sra RNAi* transgene to knockdown *sra* expression in the muscle. We applied PhTx to animals that expressed *UAS-sra RNAi* in the muscle using the GAL4 driver, *BG57-GAL4*. Surprisingly, in contrast to the dual-tissue knockdown, postsynaptic knockdown of *sra* completely blocked the rapid induction of PHP, resulting in significantly

decreased EPSP amplitudes and a failure to show a compensatory increase in quantal content (**Figure 2B,C** and **Supplementary Table 2**).

We tested the if the postsynaptic knockdown of *sra* would also result in a block of the chronic maintenance of PHP. To chronically challenge synapses, we used the *GluRIIA*^{SP16} null mutants that show robust PHP (Petersen et al., 1997). Knockdown of *sra* postsynaptically in a *GluRIIA*^{SP16} background not only exhibited an expected decrease in mEPSP amplitude compared to non-*GluRIIA*^{SP16} controls, but also a marked decrease in EPSP amplitude (**Figure 2E,F** and **Supplementary Table 2**). There was a slight but significant increase in quantal content, which likely indicates partially intact chronic PHP mechanisms (**Figure 2G**).

Our results are consistent with the idea that the knockdown of *sra* postsynaptically induces a complete block when acutely challenged, but only a partial block when chronically challenged. This suggests that the postsynaptic expression of *sra* may have a differential role in regulating these two overlapping yet functionally separable phases of PHP.

Postsynaptic *sra* overexpression blocks the maintenance of PHP but not induction

After showing that postsynaptic *sra* knockdown resulted in a strong acute block but only a partial chronic block, we examined overexpression of *sra* postsynaptically. We found that applying PhTx to synapses with *sra* overexpressed postsynaptically partially blocks PHP induction (**Figure 3A-D** and **Supplementary Table 3**). There was no significant difference in EPSPs between unchallenged and challenged NMJs. There was a small numerical increase in quantal content, but this increase did not achieve statistical significance (**Figure 3C**).

Next, we tested if postsynaptic overexpression of *sra* could block chronic PHP using the *sra*^{EY07182} allele in a *GluRIIA*^{SP16} background. Overexpressing *sra* postsynaptically showed normal EPSP amplitude (as in Figure 1), but the overexpression of *sra* in *GluRIIA*^{SP16} null NMJs displayed a significant decrease in EPSP amplitude along with a failure to increase quantal content when compared to the unchallenged control (**Figure 3E-H** and **Supplementary Table 3**), in fact the quantal content got significantly decreased in the *GluRIIA*^{SP16} background. This is indicative a strong block of chronic PHP.

Taken together, our data suggest that postsynaptic expression of *sra* is critical for different phases of PHP. Genetic *sra* knockdown or overexpression postsynaptically resulted in varying degrees of PHP block specific to the length of the challenge (acute vs. chronic). Since the postsynaptic overexpression phenotype was so strong, we checked if it correlated with NMJ developmental defects.

Postsynaptic *sra* overexpression does not impair synapse development

To test if the impairments in PHP resulting from postsynaptic overexpression of *sra* were due to impaired NMJ development, we immunostained third instar larval *Drosophila* NMJs. We overexpressed *sra* postsynaptically alone and or in conjunction with $GluRIIA^{SP16}$, matching our electrophysiological assays. We visualized NMJ bouton development in synapse 6/7 muscle segments A2 and A3 by co-staining with anti-Synapsin (Syn, presynaptic vesicle marker) and anti-Discs Large (DLG, postsynaptic density marker).

We did not find any significant differences in bouton number between any group for NMJ 6/7 within segment A2 or segment A3 (**Figure 4A-G** and **Supplementary Table 4**) (segments analyzed separately due to documented differences in development). We quantified bouton normalized per muscle area and found that postsynaptic overexpression of *sra* resulted in a significant increase compared to other genotypes (**Figure 4H** and **Supplementary Table 4**). This indicates that *sra* overexpression in the muscle may result in smaller muscles, but in any case, these unchallenged animals had intact physiology (**Figure 3**). These data indicate that postsynaptic overexpression of *sra* does not strongly impair NMJ development, and therefore, a developmental defect unlikely to be contributing towards the observed PHP block by electrophysiology.

Knockdown of *sra* presynaptically impedes the maintenance of PHP but not induction

Because we saw strong tissue-specific phenotypes when genetically dysregulating *sra* in the muscle, we wanted to test if knockdown of *sra* presynaptically also affected PHP. Acute application of PhTx to NMJs with *sra* neuronal knockdown did not block PHP induction as

EPSP amplitudes were mostly maintained, and quantal content was significantly increased between challenged and unchallenged animals (**Figure 5A-D** and **Supplementary Table 5**).

To understand if decreasing *sra* expression presynaptically blocks chronic PHP, we turned to the *GluRIIA*^{SP16} null mutant again. We found that decreased *sra* expression neuronally blocked chronic PHP because of decreased EPSP amplitude in *GluRIIA*^{SP16}, *sra RNAi* NMJs when compared to *GluRIIA*^{SP16} or *sra RNAi* alone (**Figure 5E-H** and **Supplementary Table 5**). The *GluRIIA*^{SP16}, *sra RNAi* synapses also failed to show a significant increase in quantal content compared to the unchallenged control (**Figure 5G**). This provides us with evidence that the knockdown of *sra* presynaptically blocks the long-term maintenance phase of PHP

Overexpression of *sra* presynaptically blocks PHP maintenance

Finally, we tested if the presynaptic overexpression of *sra* blocked either phase of PHP. After applying PhTx to NMJs with *sra* neuronal overexpression, we did not find any significant differences in evoked amplitude while getting a robust increase in quantal content (**Figure 6A-D** and **Supplementary Table 6**). But we tested chronic PHP following neuronal overexpression, we found a partial block. There was a statistically significant decrease in the evoked amplitudes of both the control and *sra*^{EY07182} synapses, but quantal content only showed a significant increase in the control synapses (**Figure 6E-H** and **Supplementary Table 6**). While homozygous *GluRIIA*^{SP16} null mutant NMJs do not consistently sustain evoked amplitudes perfectly (**Figure 6F**), they do consistently show a robust increase in quantal content (**Figure 6G**), which is indicative of intact chronic PHP mechanisms (Brusich et al., 2015, Frank et al., 2006, Spring et al., 2016, Yeates et al., 2017, James et al., 2019, Frank et al., 2009). This makes it unclear if there is a weak chronic block following *sra* overexpression or no block.

Taking all single-tissue electrophysiology together, our data suggest that changes in the expression of *sra* presynaptically blocks chronic PHP either strongly following *sra* RNAi or weakly following *sra* OE, while the rapid induction of PHP remains unaffected in both contexts. This provides further evidence that *sra* is required both pre- and postsynaptically to allow PHP to function normally. Additionally, the data discussed provide a compelling argument that the induction and chronic phases of PHP are functionally separable and do not completely overlap.

FK506 reverses the effects of postsynaptic overexpression of *sra*

We were puzzled why the single-tissue genetic manipulations of *sra* yielded stronger PHP inhibition. One possibility is that for instances where a molecule normally functions in multiple tissues, synapses could engage homeostatic balancing systems to cope with a global loss (e.g., endogenous genetic mutation) of that molecule. In principle, challenging a synapse with single tissue genetic manipulation could disrupt such a balance.

Our earlier experiments showed a strong chronic PHP block when *sra* was overexpressed postsynaptically (**Figure 3E-H** and **Supplementary Table 3**). We hypothesize that this may be due to an imbalance of calcineurin activity between the pre- and postsynaptic compartments. Sra is a calcineurin inhibitor. Thus, overexpressing the *sra* gene (*sra* OE) postsynaptically should decrease calcineurin activity in muscle. If the above model is correct, then impairing calcineurin globally via a pharmacological calcineurin inhibitor could restore calcineurin balance and reverse the chronic PHP block.

FK506 (tacrolimus) is a calcineurin inhibiting drug that binds to FK-binding protein l (Liu et al., 1991, Sigal and Dumont, 1992, Clardy, 1995). This immunophilin-drug binds to calcineurin and inhibits its protein phosphatase activity (Kuromi et al., 1997, Clardy, 1995, Swanson et al., 1992). There are notable phenotypes at synaptic preparations. For whole-cell patch clamp in rat cortex, application of FK506 increased the frequency of spontaneous events (Victor et al., 1995). And application of FK506 to *Drosophila* larval neuromuscular junctions has been reported to increase the endocytosis of synaptic vesicles, while having no effect on the frequency of spontaneous events or the mean amplitude of evoked events (Kuromi et al., 1997).

We repeated the experiment of overexpressing *sra* in the muscle, this time incubating NMJ preps with FK506. Larval preps were incubated with 50µM FK506 for 15 minutes prior to electrophysiological recordings. We replicated our earlier finding that *sra* muscle overexpression challenged with the $GluRIIA^{SP16}$ null mutation showed decreased evoked amplitude and a failure to increase quantal content (**Figure 7B,C** and **Supplementary Table 7**). However, when genetically identical animals were incubated with FK506, we found that EPSP amplitude is significantly increased compared to non-drugged controls, and this is a result of increased

quantal content (**Figure 7A-D** and **Supplementary Table 7**). Incubation of FK506 did not completely restore EPSPs to wild-type levels, but this experiment suggests that global inhibition of calcineurin across tissues can mitigate the chronic PHP block caused by single-tissue *sra* manipulation. Alternatively, our results may point toward non-specific potentiation presynaptically, induced by FK506. Therefore, we conducted further tests.

FK506 reverses the effects of presynaptic knockdown of *sra*

We wondered if we could reverse other PHP defects by pharmacologically blocking calcineurin. We saw a block in chronic PHP following *sra* knockdown presynaptically (**Figure 5E-H**). We repeated this experiment while also including synapses incubated with FK506. As before, in the drug-free condition, EPSP amplitudes were deficient following *sra* presynaptic knockdown challenged via $GluRIIA^{SP16}$ and failed to increase quantal content (**Figure 8B,C**). However, incubation with FK506 significantly increased EPSP amplitude in these animals, and this was accompanied by a robust increase in quantal content (**Figure 8A-D** and **Supplementary Table 8**). This provides further support that inhibition of calcineurin in a non-tissue-specific pharmacological manner can reverse defects resulting from single tissue *sra* impairments and restore PHP.

Pharmacological inhibition of calcineurin generally improves homeostatic capabilities in response to chronic PHP challenge

Finally, we tested if the pharmacological inhibition of calcineurin alone would also block PHP. We applied FK506 to $GluRIIA^{SP16}$ animals at either 10µM or 50µM concentrations. We saw no change in EPSP amplitude in wild type animals with drug application at either concentration, but interestingly, in $GluRIIA^{SP16}$ animals, we saw an increase in EPSP amplitude and quantal content following 50µM FK506 incubation compared to non-drugged controls (**Figure 9B** and **Supplementary Table 9**). The 50µM concentration also produced increases in mEPSP frequency in both wild type and $GluRIIA^{SP16}$ animals (**Figure 9D** and **Supplementary Table9**). These data are consistent with our hypothesis that global inhibition of calcineurin may create scenarios at the NMJ that are favorable to the expression of PHP.

We tested if FK506 increases release probability on its own. To do this, we conducted a failure analysis in very low calcium (0.10mM) (Frank et al., 2006, Petersen et al., 1997). In extremely low calcium, many presynaptic events fail to release vesicles and therefore fail to generate an EPSP. In these low calcium conditions, probability of vesicle release is low (Del Castillo and Katz, 1954). Our failure analysis on wild-type and *GluRIIA*^{SP16} animals with and without FK506 incubation showed that FK506 significantly decreases the number of failures compared to non-drugged controls (**Figure 9E** and **Supplementary Table 9**). Additionally, successful evoked events were significantly bigger in amplitude (on average) after FK506 incubation compared to non-drugged controls (**Figure 9F**). Taken together, these data suggest that FK506 increases release probability. This may be occurring because of calcineurin inhibition increasing presynaptic calcium either via influx from voltage-gated channels or efflux via intracellular stores.

As shown in our failure analysis experiment, FK506 can increase the EPSP amplitude in wild-type animals in low calcium (**Figure 9F** and **Supplementary Table 9**) while there were no changes at our standard calcium concentration of 0.5mM (**Figure 9B**). It is possible that at our standard calcium concentration, we are having a “ceiling effect” where the application of FK506 may not be able to increase the EPSPs any further due to electromotive driving forces. To test this idea, we conducted an experiment in 0.20mM Ca^{2+} in both wild type and *GluRIIA*^{SP16} animals with and without FK506. As we predicted, the lower calcium concentration allowed us to detect an increase in evoked amplitude and quantal content in both genotypes following incubation with FK506 (**Figure 9H,I** and **Supplementary Table 9**). This supports the idea that pharmacological calcineurin inhibition may be potentiating calcium levels to increase release probability.

DISCUSSION

In this study, we provide a new framework for understanding how individual proteins from different synaptic tissues contribute to phases of PHP. This is key to understanding how overall synaptic stability is maintained through different compensatory PHP processes in response to both acute and chronic challenges.

We show that concurrent neuronal and muscle knockdown or overexpression of *sra* does not strongly impair either acute or chronic homeostatic mechanisms (**Figure 1**). However, impairing *sra* in a tissue specific manner led to numerous blocks in either phase of PHP. Postsynaptic knockdown of *sra* disrupted acute PHP (**Figure 2**) while postsynaptic overexpression blocked chronic PHP (**Figure 3**). For the neuron, we saw the opposite effects: presynaptic knockdown of *sra* blocked chronic PHP **(Figure 5**) while presynaptic overexpression impaired acute PHP (**Figure 6**). Additionally, we were able to alleviate observed PHP blocks by pharmacologically inhibiting calcineurin via FK506 (**Figures 7, 8**). These data are consistent with a model that the relative balance of calcineurin function at NMJ tissues may control homeostatic signaling capacity. We believe that impairing *sra* either pre- or postsynaptically (separately) leads to a PHP block as it can impair the balance of calcineurin activity between the two sides of the synapse. This idea may explain why a combined pre- and postsynaptic *sra* impairment may not block PHP – even though calcineurin activity is changed, the changes are relatively balanced between both neuron and muscle. This maintains a balance of calcineurin activity between both sides of the synapse.

Potential neuronal mechanisms for *sra* regulation of calcineurin to impact PHP

Calcineurin regulation is the most notable function of *sra*. Decreased expression of *sra* increases calcineurin activity, while increased *sra* via overexpression is presumed to decrease it (Chang et al., 2003, Shaw and Chang, 2013). Our suggests that an optimal amount of *sra* expression underlies multiple different functions, each of which is necessary for robust homeostatic signaling.

Calcineurin has several presynaptic roles in various models that have been shown including affecting synaptic vesicle exocytosis and endocytosis, axon remodeling and regulating neurotransmitter release (Tarasova et al., 2018). One target of presynaptic calcineurin is to dephosphorylate synapsin 1 which can affect the mobilization of synaptic vesicles from the reserve pool to active zones (Cesca et al., 2010, Jovanovic et al., 2001, Chi et al., 2003). For those studies, opposing interactions between calcineurin and various kinases regulate vesicle mobilization. This may explain why neuronal *sra* overexpression impaired acute PHP because increased *sra* decreases calcineurin activity which may impair the mobilization of vesicles to

active zones. Challenges to NMJ function (e.g., *GluRIIA*^{SP16} or PhTx) consistently increase the number of vesicles that are released, and failure to mobilize enough vesicles in response to a challenge may lead to a failure for compensatory quantal content increase and impair evoked release.

There are conflicting results on how the use of calcineurin inhibitors affects exocytosis. They have been shown to increase the rate of exocytosis, show no change at all, or suppress exocytosis (Yakel, 1997, Sim et al., 2003, Kumashiro et al., 2005). Specifically in the *Drosophila* NMJ, calcineurin inhibition via FK506 has been shown to increase the endocytosis of synaptic vesicles, while having no effect on the frequency of spontaneous events or the mean amplitude of evoked events (Kuromi et al., 1997). This is contrary to the results of the current study where we showed that mEPSP frequency is increased following FK506 incubation (**Figure 9D**). This difference may be explained by the differences in concentration of FK506 that was used as previously, only 5µM and 10µM were tested. We see no change in mEPSP frequency at 10µM FK506, like previous work as we only see the increase in spontaneous event frequency following 50µM FK506.

Calcineurin is believed to be a calcium-dependent regulator of endocytosis at both neuronal and non-neuronal secretory cells (Wu et al., 2014). Calcineurin inhibitors slow endocytosis in response to a small calcium influx but does not alter the speed of endocytosis in response to a large calcium influx. If calcineurin is inhibiting synaptic vesicle recycling, this may explain why we see a defect in chronic PHP following neuronal *sra* knockdown. Knockdown of *sra* leads to increased calcineurin activity, and therefore increase inhibition of vesicular recycling. While this may not lead to abnormal neurotransmission in the absence of a challenge, evoked amplitude may not be maintained when chronically challenged due to an increased need for vesicle recycling in response to the challenge.

Calcineurin may be affecting calcium influx as the targets of calcineurin in mouse NMJ are L-type calcium channels (Gaydukov et al., 2013). Specifically, it was shown that calcineurin downregulates neurotransmitter release by suppressing L-type calcium channels and calcium release from intracellular stores through ryanodine receptors. In the *Drosophila* NMJ, it has recently been shown that while L-type calcium channels are localized around active zones and contribute to AP-triggered calcium influx, they are dispensable for evoked release (Krick et al.,

2021). However, it has not been shown if these channels are necessary for homeostatic signaling processes. Calcium influx increases in response to both acute and chronic challenges to the synapse (Müller and Davis, 2012). L-type calcium channels may be necessary for homeostatic compensation as they not only serve as an additional entry point of calcium into the presynaptic compartment to contribute to neurotransmitter release, but calcium entry through these channels also induces calcium release from intracellular stores. In the current study, presynaptic overexpression of *sra* leads to increased calcineurin which may lead to increased inhibition of L-type calcium channels and not allow for a large enough compensatory increase in calcium influx necessary to respond to a homeostatic challenge.

Possible postsynaptic mechanisms of *sra* to PHP through calcineurin regulation

We showed that postsynaptic *sra* knockdown impaired acute homeostatic signaling (**Figure 2**) while postsynaptic *sra* overexpression strongly blocked chronic homeostatic signaling (**Figure 3**). It is well known that postsynaptically, calcineurin activation can lead to the dephosphorylation of AMPA receptors that can lead to the internalization of them (D'Amelio et al., 2011, He et al., 2009, Lin et al., 2000). The ionotropic glutamate receptors that are localized to muscle in *Drosophila* are *DGluRIIA* and *DGluRIIB*, both of which are AMPA/kainite type receptors (Betz et al., 1993, Petersen et al., 1997). This presents a potential mechanism for how *sra* knockdown in the muscle blocks PHP- decreased *sra* expression increases calcineurin activity which may lead to increased internalization of postsynaptic glutamate receptors. A decrease in the amount of available glutamate receptors may be detrimental when glutamate receptors are already being challenged via philanthotoxin.

One theory for how postsynaptic *sra* overexpression blocks chronic PHP is through its interaction with CaMKII. Calcineurin dephosphorylates and I-1 which activates PPI to in turn dephosphorylate and inactivate CaMKII (Tarasova et al., 2018). In the *Drosophila* NMJ, pCaMKII levels have been found to be decreased following genetic glutamate receptor impairment (Newman et al., 2017, Li et al., 2018, Goel et al., 2017). Overexpression of *sra* increases calcineurin which may lead to an increased amount of pCaMKII, contrary to what normally occurs in response to a homeostatic challenge. While it is unclear if *sra* is linked to the

ability of CaMKII to regulate PHP, it will be interesting to test potential links along with understanding how decreased pCaMKII contributes to PHP.

How *sra* may affect PHP through non-calcineurin regulating roles

Previous work in rat cortex suggests that RCAN1 expression is upregulated following incubation with Aβ (Lloret et al., 2011). The authors proposed that RCAN1 proteins not only inhibits calcineurin but can also shift tau to a hyperphosphorylated state via inducing expression of GSK3β. This provides evidence that RCAN1 proteins are linked to Alzheimer's and neurodegeneration. Like this work and human studies, Aβ42-expressing *Drosophila* show increased Sra levels in the brain (Lee et al., 2016). Genetic overexpression of *sra* in combination with Aβ42 impaired locomotor activity and lifespan compared to overexpression of *sra* alone. However, data from *Drosophila* suggest that upregulation of *sra* can be neuroprotective in the presence of amyloid precursor protein (APP) by facilitating the transport of synaptic proteins and mitochondria (Shaw and Chang, 2013). These conflicting results regarding the overexpression of *sra* demonstrate that *sra* is involved with both APP and Aβ42 separate from its function of regulating calcineurin. It is unclear if *sra* is working through calcineurin, APP, Aβ42 or other molecules to contribute to both pre- and postsynaptic homeostatic signaling processes. This line of research may also lead to examining other open questions such as how defective homeostatic synaptic processes may contribute to neurodegeneration and other neural pathologies. It is known that most genes that are necessary for PHP are linked to neural disorders and pathologies such as autism spectrum disorders, schizophrenia, Fragile X Syndrome, migraine, and epilepsy (Wondolowski and Dickman, 2013, Frank et al., 2020).

Another idea for how the expression of *sra* may be regulating PHP is through its effects on mitochondrial function. Both increases and decreases in *sra* have been shown to result in decreased ATP levels, increased ROS production, decreased mitochondrial DNA in *Drosophila* heads, decreased mitochondrial size, and increased mitochondrial number (Chang and Min, 2005). This is independent from its function of regulating calcineurin as decreasing calcineurin activity in *sra* mutants did not rescue mitochondrial enzymatic activity. Recent work also indicates that Mitochondrial Complex I (MCI) is necessary for synapse function and plasticity at the *Drosophila* NMJ (Mallik and Frank, 2022). Genetic knockdown or pharmacological

inhibition of MCI impaired neurotransmission, reduced NMJ growth and altered NMJ morphology.

Acute versus chronic PHP expression with single tissue contributions

There is strong evidence to suggest that there are shared mechanisms underlying both the acute and chronic forms of PHP signaling as both forms display robust increases in readily releasable pool (RRP) size and Ca_V2-mediated calcium influx that result in increases in quantal content necessary for function PHP(Davis and Müller, 2015, Müller and Davis, 2012). Recent work has found that the acute and chronic forms of PHP are functionally separable (James et al., 2019). Our data support this idea by showing minimal overlap in a specific *sra* impairment in a specific tissue. For example, *sra* knockdown postsynaptically only blocked acute PHP while leaving the chronic phase intact; conversely, *sra* overexpression postsynaptically did not impair acute PHP while blocking chronic PHP. These data demonstrate that *sra* is tightly regulated as both too much and too little sra can disrupt PHP. Importantly, these data support the separation of acute and chronic PHP as *sra* expression is likely regulating different processes at different timepoints that integrate to produce functional PHP. Other work has suggested that PHP pathways converge onto the same targets (Goel et al., 2017). While it is possible that discrete signaling pathways converge, it is more likely that there is some degree of convergence while also some amount of separate signaling systems. It will be important for future studies to test how the individual influences of molecules from distinct synaptic tissues underly the different phases of PHP to promote a fully functional PHP signaling system.

References

ANDRE, E. A., FORCELLI, P. A. & PAK, D. T. 2018. What goes up must come down: homeostatic synaptic plasticity strategies in neurological disease. *Future Neurol,* 13**,** 13-21.

BAUMGÄRTEL, K. & MANSUY, I. M. 2012. Neural functions of calcineurin in synaptic plasticity and memory. *Learn Mem,* 19**,** 375-84.

BETZ, H., SCHUSTER, C., ULTSCH, A. & SCHMITT, B. 1993. Molecular biology of ionotropic glutamate receptors in Drosophila melanogaster. *Trends in Pharmacological Sciences,* 14**,** 428-431.

BLISS, T. V. P., COLLINGRIDGE, G. L. & MORRIS, R. G. M. 2014. Synaptic plasticity in health and disease: introduction and overview. *Philosophical Transactions of the Royal Society B: Biological Sciences,* 369**,** 20130129.

BÖHME, M. A., MCCARTHY, A. W., GRASSKAMP, A. T., BEUSCHEL, C. B., GOEL, P., JUSYTE, M., LABER, D., HUANG, S., REY, U., PETZOLDT, A. G., LEHMANN, M., GÖTTFERT, F., HAGHIGHI, P., HELL, S. W., OWALD, D., DICKMAN, D., SIGRIST, S. J. & WALTER, A. M. 2019. Rapid active zone remodeling consolidates presynaptic potentiation. *Nature Communications,* 10**,** 1085.

BRUSICH, D. J., SPRING, A. M. & FRANK, C. A. 2015. A single-cross, RNA interference-based genetic tool for examining the long-term maintenance of homeostatic plasticity. *Front Cell Neurosci,* 9**,** 107.

BUDNIK, V., KOH, Y. H., GUAN, B., HARTMANN, B., HOUGH, C., WOODS, D. & GORCZYCA, M. 1996. Regulation of synapse structure and function by the Drosophila tumor suppressor gene dlg. *Neuron,* 17**,** 627-40.

CESCA, F., BALDELLI, P., VALTORTA, F. & BENFENATI, F. 2010. The synapsins: key actors of synapse function and plasticity. *Prog Neurobiol,* 91**,** 313-48.

CHANG, K. T. & MIN, K. T. 2005. Drosophila melanogaster homolog of Down syndrome critical region 1 is critical for mitochondrial function. *Nat Neurosci,* 8**,** 1577-85.

CHANG, K. T., SHI, Y.-J. & MIN, K.-T. 2003. The Drosophila homolog of Down's syndrome critical region 1 gene regulates learning: Implications for mental retardation. *Proceedings of the National Academy of Sciences,* 100**,** 15794-15799.

CHI, P., GREENGARD, P. & RYAN, T. A. 2003. Synaptic vesicle mobilization is regulated by distinct synapsin I phosphorylation pathways at different frequencies. *Neuron,* 38**,** 69-78.

CLARDY, J. 1995. The chemistry of signal transduction. *Proceedings of the National Academy of Sciences of the United States of America,* 92**,** 56-61.

D'AMELIO, M., CAVALLUCCI, V., MIDDEI, S., MARCHETTI, C., PACIONI, S., FERRI, A., DIAMANTINI, A., DE ZIO, D., CARRARA, P., BATTISTINI, L., MORENO, S., BACCI, A., AMMASSARI-TEULE, M., MARIE, H. & CECCONI, F. 2011. Caspase-3 triggers early synaptic dysfunction in a mouse model of Alzheimer's disease. *Nat Neurosci,* 14**,** 69-76.

DAVIS, G. W. 2006. Homeostatic control of neural activity: from phenomenology to molecular design. *Annu Rev Neurosci,* 29**,** 307-23.

DAVIS, G. W., DIANTONIO, A., PETERSEN, S. A. & GOODMAN, C. S. 1998. Postsynaptic PKA controls quantal size and reveals a retrograde signal that regulates presynaptic transmitter release in Drosophila. *Neuron,* 20**,** 305-15.

DAVIS, G. W. & MÜLLER, M. 2015. Homeostatic Control of Presynaptic Neurotransmitter Release. *Annual Review of Physiology,* 77**,** 251-270.

DEL CASTILLO, J. & KATZ, B. 1954. Quantal components of the end-plate potential. *J Physiol,* 124**,** 560-73.

DIANTONIO, A., PETERSEN, S. A., HECKMANN, M. & GOODMAN, C. S. 1999. Glutamate receptor expression regulates quantal size and quantal content at the Drosophila neuromuscular junction. *Journal of Neuroscience,* 19**,** 3023-3032.

DICKMAN, D. & WONDOLOWSKI, J. 2013. Emerging links between homeostatic synaptic plasticity and neurological disease. *Frontiers in Cellular Neuroscience,* 7.

FRANK, C. A. 2014. Homeostatic plasticity at the Drosophila neuromuscular junction. *Neuropharmacology,* 78**,** 63-74.

FRANK, C. A., JAMES, T. D. & MÜLLER, M. 2020. Homeostatic control of Drosophila neuromuscular junction function. *Synapse,* 74**,** e22133.

FRANK, C. A., KENNEDY, M. J., GOOLD, C. P., MAREK, K. W. & DAVIS, G. W. 2006. Mechanisms underlying the rapid induction and sustained expression of synaptic homeostasis. *Neuron,* 52**,** 663-77.

FRANK, C. A., PIELAGE, J. & DAVIS, G. W. 2009. A presynaptic homeostatic signaling system composed of the Eph receptor, ephexin, Cdc42, and CaV2.1 calcium channels. *Neuron,* 61**,** 556-69.

FURMAN, J. L. & NORRIS, C. M. 2014. Calcineurin and glial signaling: neuroinflammation and beyond. *J Neuroinflammation,* 11**,** 158.

GAYDUKOV, A., TARASOVA, E. & BALEZINA, O. 2013. Calcium-dependent phosphatase calcineurin downregulates evoked neurotransmitter release in neuromuscular junctions of mice. *Neurochemical Journal,* 7**,** 29-33.

GOEL, P., LI, X. & DICKMAN, D. 2017. Disparate Postsynaptic Induction Mechanisms Ultimately Converge to Drive the Retrograde Enhancement of Presynaptic Efficacy. *Cell Rep,* 21**,** 2339-2347.

GREENSPAN, R. J. 2004. *Fly pushing : the theory and practice of Drosophila genetics,* Cold Spring Harbor, N.Y., Cold Spring Harbor Laboratory Press.

HARRIS, C. D., ERMAK, G. & DAVIES, K. J. 2005. Multiple roles of the DSCR1 (Adapt78 or RCAN1) gene and its protein product calcipressin 1 (or RCAN1) in disease. *Cell Mol Life Sci,* 62**,** 2477-86.

HARRIS, N., BRAISER, D. J., DICKMAN, D. K., FETTER, R. D., TONG, A. & DAVIS, G. W. 2015. The Innate Immune Receptor PGRP-LC Controls Presynaptic Homeostatic Plasticity. *Neuron,* 88**,** 1157-64.

HAZELRIGG, T., LEVIS, R. & RUBIN, G. M. 1984. Transformation of white locus DNA in drosophila: dosage compensation, zeste interaction, and position effects. *Cell,* 36**,** 469-81.

HE, K., SONG, L., CUMMINGS, L. W., GOLDMAN, J., HUGANIR, R. L. & LEE, H.-K. 2009. Stabilization of Ca^{2+}-permeable AMPA receptors at perisynaptic sites by GluR1-S845 phosphorylation. *Proceedings of the National Academy of Sciences,* 106**,** 20033-20038.

HORNER, V. L., CZANK, A., JANG, J. K., SINGH, N., WILLIAMS, B. C., PURO, J., KUBLI, E., HANES, S. D., MCKIM, K. S., WOLFNER, M. F. & GOLDBERG, M. L. 2006. The Drosophila Calcipressin Sarah Is Required for Several Aspects of Egg Activation. *Current Biology,* 16**,** 1441-1446.

JAMES, T. D., ZWIEFELHOFER, D. J. & FRANK, C. A. 2019. Maintenance of homeostatic plasticity at the Drosophila neuromuscular synapse requires continuous IP3-directed signaling. *eLife,* 8.

JAN, L. Y. & JAN, Y. N. 1976. Properties of the larval neuromuscular junction in Drosophila melanogaster. *The Journal of physiology,* 262**,** 189-214.

JOVANOVIC, J. N., SIHRA, T. S., NAIRN, A. C., HEMMINGS, H. C., JR., GREENGARD, P. & CZERNIK, A. J. 2001. Opposing changes in phosphorylation of specific sites in synapsin I during Ca2+-dependent glutamate release in isolated nerve terminals. *J Neurosci,* 21**,** 7944-53.

KADAMUR, G. & ROSS, E. M. 2013. Mammalian phospholipase C. *Annu Rev Physiol,* 75**,** 127-54.

KIKUMA, K., LI, X., PERRY, S., LI, Q., GOEL, P., CHEN, C., KIM, D., STAVROPOULOS, N. & DICKMAN, D. 2019. Cul3 and insomniac are required for rapid ubiquitination of postsynaptic targets and retrograde homeostatic signaling. *Nature Communications,* 10**,** 2998.

KINGSBURY, T. J. & CUNNINGHAM, K. W. 2000. A conserved family of calcineurin regulators. *Genes & development,* 14**,** 1595-1604.

KRICK, N., RYGLEWSKI, S., PICHLER, A., BIKBAEV, A., GÖTZ, T., KOBLER, O., HEINE, M., THOMAS, U. & DUCH, C. 2021. Separation of presynaptic Ca_v2 and Ca_v1 channel function in synaptic vesicle exo- and endocytosis by the membrane anchored Ca^{2+} pump PMCA. *Proceedings of the National Academy of Sciences,* 118**,** e2106621118.

KUMASHIRO, S., LU, Y. F., TOMIZAWA, K., MATSUSHITA, M., WEI, F. Y. & MATSUI, H. 2005. Regulation of synaptic vesicle recycling by calcineurin in different vesicle pools. *Neurosci Res,* 51**,** 435-43.

KUROMI, H., YOSHIHARA, M. & KIDOKORO, Y. 1997. An inhibitory role of calcineurin in endocytosis of synaptic vesicles at nerve terminals of Drosophila larvae. *Neurosci Res,* 27**,** 101-13.

LEE, J. I., DHAKAL, B. K., LEE, J., BANDYOPADHYAY, J., JEONG, S. Y., EOM, S. H., KIM, D. H. & AHNN, J. 2003. The Caenorhabditis elegans Homologue of Down Syndrome Critical Region 1, RCN-1, Inhibits Multiple Functions of the Phosphatase Calcineurin. *Journal of Molecular Biology,* 328**,** 147-156.

LEE, S., BANG, S. M., HONG, Y. K., LEE, J. H., JEONG, H., PARK, S. H., LIU, Q. F., LEE, I. S. & CHO, K. S. 2016. The calcineurin inhibitor Sarah (Nebula) exacerbates Abeta42 phenotypes in a Drosophila model of Alzheimer's disease. *Dis Model Mech,* 9**,** 295-306.

LI, X., GOEL, P., CHEN, C., ANGAJALA, V., CHEN, X. & DICKMAN, D. K. 2018. Synapse-specific and compartmentalized expression of presynaptic homeostatic potentiation. *eLife,* 7**,** e34338.

LIN, D. M. & GOODMAN, C. S. 1994. Ectopic and increased expression of Fasciclin II alters motoneuron growth cone guidance. *Neuron,* 13**,** 507-23.

LIN, J. W., JU, W., FOSTER, K., LEE, S. H., AHMADIAN, G., WYSZYNSKI, M., WANG, Y. T. & SHENG, M. 2000. Distinct molecular mechanisms and divergent endocytotic pathways of AMPA receptor internalization. *Nat Neurosci,* 3**,** 1282-90.

LIU, J., FARMER, J. D., JR., LANE, W. S., FRIEDMAN, J., WEISSMAN, I. & SCHREIBER, S. L. 1991. Calcineurin is a common target of cyclophilin-cyclosporin A and FKBP-FK506 complexes. *Cell,* 66**,** 807-15.

LLORET, A., BADIA, M. C., GIRALDO, E., ERMAK, G., ALONSO, M. D., PALLARDÓ, F. V., DAVIES, K. J. & VIÑA, J. 2011. Amyloid-β toxicity and tau hyperphosphorylation are linked via RCAN1 in Alzheimer's disease. *J Alzheimers Dis,* 27**,** 701-9.

MALLIK, B. & FRANK, C. A. 2022. Roles for Mitochondrial Complex I Subunits in Regulating Synaptic Transmission and Growth. *Frontiers in Neuroscience,* 16.

MARDER, E. 2012. Neuromodulation of neuronal circuits: back to the future. *Neuron,* 76**,** 1-11.

MENON, K. P., CARRILLO, R. A. & ZINN, K. 2013. Development and plasticity of the Drosophila larval neuromuscular junction. *Wiley Interdiscip Rev Dev Biol,* 2**,** 647-70.

MÜLLER, M. & DAVIS, G. W. 2012. Transsynaptic control of presynaptic Ca^{2+} influx achieves homeostatic potentiation of neurotransmitter release. *Current biology : CB,* 22**,** 1102-1108.

MÜLLER, M., GENÇ, Ö. & DAVIS, G. W. 2015. RIM-Binding Protein Links Synaptic Homeostasis to the Stabilization and Replenishment of High Release Probability Vesicles. *Neuron,* 85**,** 1056-69.

MÜLLER, M., LIU, K. S., SIGRIST, S. J. & DAVIS, G. W. 2012. RIM Controls Homeostatic Plasticity through Modulation of the Readily-Releasable Vesicle Pool. *J Neurosci,* 32**,** 16574-85.

MUSSON, R. E. & SMIT, N. P. 2011. Regulatory mechanisms of calcineurin phosphatase activity. *Curr Med Chem,* 18**,** 301-15.

NAIR, A. G., MUTTATHUKUNNEL, P. & MÜLLER, M. 2021. Distinct molecular pathways govern presynaptic homeostatic plasticity. *Cell Rep,* 37**,** 110105.

NAKAI, Y., HORIUCHI, J., TSUDA, M., TAKEO, S., AKAHORI, S., MATSUO, T., KUME, K. & AIGAKI, T. 2011. Calcineurin and its regulator sra/DSCR1 are essential for sleep in Drosophila. *J Neurosci,* 31**,** 12759-66.

NEWMAN, Z. L., HOAGLAND, A., AGHI, K., WORDEN, K., LEVY, S. L., SON, J. H., LEE, L. P. & ISACOFF, E. Y. 2017. Input-Specific Plasticity and Homeostasis at the Drosophila Larval Neuromuscular Junction. *Neuron,* 93**,** 1388-1404.e10.

PARK, J., OH, Y. & CHUNG, K. C. 2009. Two key genes closely implicated with the neuropathological characteristics in Down syndrome: DYRK1A and RCAN1. *BMB Rep,* 42**,** 6-15.

PETERSEN, S. A., FETTER, R. D., NOORDERMEER, J. N., GOODMAN, C. S. & DIANTONIO, A. 1997. Genetic analysis of glutamate receptors in Drosophila reveals a retrograde signal regulating presynaptic transmitter release. *Neuron,* 19**,** 1237-48.

PHILIP, F., KADAMUR, G., SILOS, R. G., WOODSON, J. & ROSS, E. M. 2010. Synergistic activation of phospholipase C-beta3 by Galpha(q) and Gbetagamma describes a simple two-state coincidence detector. *Curr Biol,* 20**,** 1327-35.

POZO, K. & GODA, Y. 2010. Unraveling mechanisms of homeostatic synaptic plasticity. *Neuron,* 66**,** 337-51.

RUSNAK, F. & MERTZ, P. 2000. Calcineurin: form and function. *Physiol Rev,* 80**,** 1483-521.

SHAW, J. L. & CHANG, K. T. 2013. Nebula/DSCR1 Upregulation Delays Neurodegeneration and Protects against APP-Induced Axonal Transport Defects by Restoring Calcineurin and GSK-3β Signaling. *PLOS Genetics,* 9**,** e1003792.

SIGAL, N. H. & DUMONT, F. J. 1992. Cyclosporin A, FK-506, and rapamycin: pharmacologic probes of lymphocyte signal transduction. *Annu Rev Immunol,* 10**,** 519-60.

SIM, A. T., BALDWIN, M. L., ROSTAS, J. A., HOLST, J. & LUDOWYKE, R. I. 2003. The role of serine/threonine protein phosphatases in exocytosis. *Biochem J,* 373**,** 641-59.

SPRING, A. M., BRUSICH, D. J. & FRANK, C. A. 2016. C-terminal Src Kinase Gates Homeostatic Synaptic Plasticity and Regulates Fasciclin II Expression at the Drosophila Neuromuscular Junction. *PLOS Genetics,* 12**,** e1005886.

STEWART, B., ATWOOD, H., RENGER, J., WANG, J. & WU, C. 1994. Improved stability of Drosophila larval neuromuscular preparations in haemolymph-like physiological solutions A Neuroethology, sensory, neural, and behavioral physiology.

SWANSON, S. K., BORN, T., ZYDOWSKY, L. D., CHO, H., CHANG, H. Y., WALSH, C. T. & RUSNAK, F. 1992. Cyclosporin-mediated inhibition of bovine calcineurin by cyclophilins A and B. *Proc Natl Acad Sci U S A,* 89**,** 3741-5.

TAKEO, S., SWANSON, S. K., NANDANAN, K., NAKAI, Y., AIGAKI, T., WASHBURN, M. P., FLORENS, L. & HAWLEY, R. S. 2012. Shaggy/glycogen synthase kinase 3beta and phosphorylation of Sarah/regulator of calcineurin are essential for completion of Drosophila female meiosis. *Proc Natl Acad Sci U S A,* 109**,** 6382-9.

TAKEO, S., TSUDA, M., AKAHORI, S., MATSUO, T. & AIGAKI, T. 2006. The Calcineurin Regulator Sra Plays an Essential Role in Female Meiosis in Drosophila. *Current Biology,* 16**,** 1435-1440.

TARASOVA, E. O., GAYDUKOV, A. E. & BALEZINA, O. P. 2018. Calcineurin and Its Role in Synaptic Transmission. *Biochemistry (Mosc),* 83**,** 674-689.

TONONI, G. & CIRELLI, C. 2006. Sleep function and synaptic homeostasis. *Sleep Medicine Reviews,* 10**,** 49-62.

VICTOR, R. G., THOMAS, G. D., MARBAN, E. & O'ROURKE, B. 1995. Presynaptic modulation of cortical synaptic activity by calcineurin. *Proceedings of the National Academy of Sciences of the United States of America,* 92**,** 6269-6273.

WANG, T., HAUSWIRTH, A. G., TONG, A., DICKMAN, D. K. & DAVIS, G. W. 2014. Endostatin is a trans-synaptic signal for homeostatic synaptic plasticity. *Neuron,* 83**,** 616-29.

WEYHERSMÜLLER, A., HALLERMANN, S., WAGNER, N. & EILERS, J. 2011. Rapid active zone remodeling during synaptic plasticity. *J Neurosci,* 31**,** 6041-52.

WONDOLOWSKI, J. & DICKMAN, D. 2013. Emerging links between homeostatic synaptic plasticity and neurological disease. *Front Cell Neurosci,* 7**,** 223.

WU, X.-S., ZHANG, Z., ZHAO, W.-D., WANG, D., LUO, F. & WU, L.-G. 2014. Calcineurin is universally involved in vesicle endocytosis at neuronal and nonneuronal secretory cells. *Cell reports,* 7**,** 982-988.

YAKEL, J. L. 1997. Calcineurin regulation of synaptic function: from ion channels to transmitter release and gene transcription. *Trends Pharmacol Sci,* 18**,** 124-34.

YEATES, C. J., ZWIEFELHOFER, D. J. & FRANK, C. A. 2017. The Maintenance of Synaptic Homeostasis at the Drosophila Neuromuscular Junction Is Reversible and Sensitive to High Temperature. *eNeuro,* 4.

YOUNGER, M. A., MÜLLER, M., TONG, A., PYM, E. C. & DAVIS, G. W. 2013. A presynaptic ENaC channel drives homeostatic plasticity. *Neuron,* 79**,** 1183-96.

Figure 1. Dual pre and postsynaptic knockdown or overexpression does not block PHP **(A-C)** quantification showing average mEPSP amplitude, EPSP amplitude, and quantal content in pre + post-GAL4 control and pre + post-GAL4 driven *sra* RNAi. Black points show DMSO control synapses, green points show synapses treated with PhTx, and magenta points show animals chronically challenged with *GluRIII* RNAi. **(D, H)** Representative electrophysiological traces of EPSPs (above) and mEPSPs (below). Scale bars for all traces are y = 10 mV (1mV), x = 20 ms (500 ms) for EPSPs (mEPSPs). **(E-G)** Quantification showing average mEPSP amplitude, EPSP amplitude, and quantal content in pre + post-GAL4 control and pre + post-GAL4 driven *sra* overexpression (OE). Black points show DMSO control synapses, green points show synapses treated with PhTx, and magenta points show animals chronically challenged with *GluRIII* RNAi. *p<0.05, **p<0.01, ***p<001 by Multiple Student's T-test and corrected for multiple comparisons using the Holm-Sidak method. DMSO controls were compared to PhTx and *GluRIII* RNAi synapses for driver controls and separately for *sra* RNAi or OE.

Figure 2. Induction of presynaptic homeostatic potentiation requires muscle expression of *sra*, but maintenance does not. **(A-C)** Quantification showing average mEPSP amplitude, EPSP amplitude, and quantal content in post-GAL4 control and post-GAL4 driven *sra* RNAi. Black points show DMSO control synapses, while green points show synapses treated with PhTx. **(D, H)** Representative electrophysiological traces of EPSPs (above) and mEPSPs (below). Scale bars for all traces are y = 10 mV (1mV), x = 20 ms (500 ms) for EPSPs (mEPSPs). **(E-G)** Quantification showing average mEPSP amplitude, EPSP amplitude, and quantal content in post-GAL4 control and post-GAL4 driven *sra* RNAi in both the presence and absence of $GluRIIA^{SP16}$. *p<0.05, **p<0.01, ***p<001 by Student's T-test versus non-challenged genetic control.

Figure 3. Maintenance of presynaptic homeostatic potentiation is impaired by muscle overexpression of *sra*, but induction is not. **(A-C)** Quantification showing average mEPSP amplitude, EPSP amplitude, and quantal content in post-GAL4 control and post-GAL4 driven *sra* overexpression (OE). Black points show DMSO control synapses, while green points show synapses treated with PhTx. **(D, H)** Representative electrophysiological traces of EPSPs (above) and mEPSPs (below). Scale bars for all traces are y = 10 mV (1mV), x = 20 ms (500 ms) for

EPSPs (mEPSPs). **(E-G)** Quantification showing average mEPSP amplitude, EPSP amplitude, and quantal content in post-GAL4 control and post-GAL4 driven *sra* OE in both the presence and absence of *GluRIIA*^{SP16}. *p<0.05, **p<0.01, ***p<001 by Student's T-test versus non-challenged genetic control.

Figure 4. Postsynaptic *sra* overexpression does not impair synapse development. **(A-F)** NMJs were co-stained with anti-DLG (magenta) and anti-Synapsin antibodies (green) to visualize synaptic boutons. **(G)** NMJ growth was assessed by bouton counting at abdominal segments A2 and A3, muscle 6/7, based on postsynaptic DLG staining and checking for presynaptic Synapsin. **(H)** Bouton counts were normalized per unit of muscle 6/7 area. Ordinary one-way ANOVAs were used to compare each genotype within each segment followed by a Tukey's HSD test for multiple comparisons. *p<0.05, **p<0.01, ***p<001.

Figure 5. Maintenance of presynaptic homeostatic potentiation is impaired by neuronal knockdown of *sra*, but induction is not. **(A-C)** Quantification showing average mEPSP amplitude, EPSP amplitude, and quantal content in pre-GAL4 control and pre-GAL4 driven *sra* RNAi. Black points show DMSO control synapses, while green points show synapses treated with PhTx. **(D, H)** Representative electrophysiological traces of EPSPs (above) and mEPSPs (below). Scale bars for all traces are y = 10 mV (1mV), x = 20 ms (500 ms) for EPSPs (mEPSPs). **(E-G)** Quantification showing average mEPSP amplitude, EPSP amplitude, and quantal content in pre-GAL4 control and pre-GAL4 driven *sra* RNAi in both the presence and absence of *GluRIIA*^{SP16}. *p<0.05, **p<0.01, ***p<001 by Student's T-test versus non-challenged genetic control.

Figure 6. Maintenance of presynaptic homeostatic potentiation is impaired by neuronal overexpression of *sra*, but induction is not. **(A-C)** Quantification showing average mEPSP amplitude, EPSP amplitude, and quantal content in pre-GAL4 control and pre-GAL4 driven *sra* overexpression (OE). Black points show DMSO control synapses, while green points show synapses treated with PhTx. **(D, H)** Representative electrophysiological traces of EPSPs (above)

and mEPSPs (below). Scale bars for all traces are y = 10 mV (1mV), x = 20 ms (500 ms) for EPSPs (mEPSPs). **(E-G)** Quantification showing average mEPSP amplitude, EPSP amplitude, and quantal content in pre-GAL4 control and pre-GAL4 driven *sra* OE in both the presence and absence of *GluRIIA*^{SP16}. *p<0.05, **p<0.01, ***p<001 by Student's T-test versus non-challenged genetic control.

Figure 7. Pharmacological inhibition of calcineurin partially rescues the PHP deficit observed in chronically challenged postsynaptic overexpression of *sra* animals. **(A-C)** Quantification showing average mEPSP amplitude, EPSP amplitude, and quantal content in post-GAL4 control and post-GAL4 driven *sra* overexpression (OE) in both the presence and absence of 50µM FK506. Black points show DMSO control synapses while dark pink points represent 50µM FK506. **(D)** Representative electrophysiological traces of EPSPs (above) and mEPSPs (below). Scale bars for all traces are y = 10 mV (1mV), x = 20 ms (500 ms) for EPSPs (mEPSPs). Two-way ANOVAs were used to compare each genotype with and without drug followed by a Tukey's HSD test for multiple comparisons. *p<0.05, **p<0.01, ***p<001.

Figure 8. Pharmacological inhibition of calcineurin rescues the PHP deficit observed in chronically challenged presynaptic knockdown of *sra* animals. **(A-C)** Quantification showing average mEPSP amplitude, EPSP amplitude, and quantal content in pre-GAL4 control and pre-GAL4 driven *sra* knockdown in both the presence and absence of 50µM FK506. Black points show DMSO control synapses while dark pink points represent 50µM FK506. **(D)** Representative electrophysiological traces of EPSPs (above) and mEPSPs (below). Scale bars for all traces are y = 10 mV (1mV), x = 20 ms (500 ms) for EPSPs (mEPSPs). Two-way ANOVAs were used to compare each genotype with and without drug followed by a Tukey's HSD test for multiple comparisons. *p<0.05, **p<0.01, ***p<001.

Figure 9. Maintenance of presynaptic homeostatic potentiation can be further potentiated by pharmacologically inhibiting calcineurin. **(A-D)** Quantification showing average mEPSP amplitude, EPSP amplitude, quantal content, and mEPSP frequency in wild type and *GluRIIA*^{SP16}

animals. Black points show 10µM DMSO control, light pink points show 10µM FK506, grey points show 50µM DMSO control, and dark pink points show 50µM FK506. **(E,F)** Quantification of failure analysis experiment. 0.10mM Ca^{2+} was used in this experiment. "% failures" represents the number of stimulation pulses that failed to elicit any discernable response out of the 100 total pulses per synapse. Black points represent DMSO control, while the dark pink points represent 50µM FK506. **(G-I)** Quantification showing average mEPSP amplitude, EPSP amplitude, and quantal content in wild type and *GluRIIA*^{SP16} animals dissected in low calcium conditions (0.20mM Ca^{2+}). Black points represent DMSO control, while the dark pink points represent 50µM FK506. *p<0.05, **p<0.01, ***p<001 by Student's T-test versus non-drugged control.

Conflict of Interest

The authors declare that the research was conducted in the absence of any commercial or financial relationships that could be construed as a potential conflict of interest.

Author Contributions

NSA and CAF designed the research, analyzed the data, and wrote the manuscript. NSA performed the research. Both authors contributed to the article and approved the submitted version.

Funding

This work was supported by a grant from the National Institutes of Health/NINDS (R01NS085164) to CAF. This work was also supported by NIN/NINDS grant supplement to NSA for grant NS085164 (PI - CAF).

Acknowledgements

We thank members of the Frank lab for helpful comments throughout this study. We thank the laboratories of Tina Tootle, Toshihiro Kitamoto, Pamela Geyer, and Lori Wallrath for helpful discussions. Additionally, we thank Drs. Samuel Young, Joshua Weiner, and Catherine Marcinkiewcz for helpful suggestions. We also thank the Bloomington Drosophila Resource Stock Center for several fly stocks detailed in the Methods section.

Supplementary Material

Supplementary Tables S1-S3 and S5-S9 show raw electrophysiology data. Table S4 shows raw bouton counts and measurements for NMJ growth assessment.

Data Availability Statement

The raw datasets for this study will be made available by the authors.

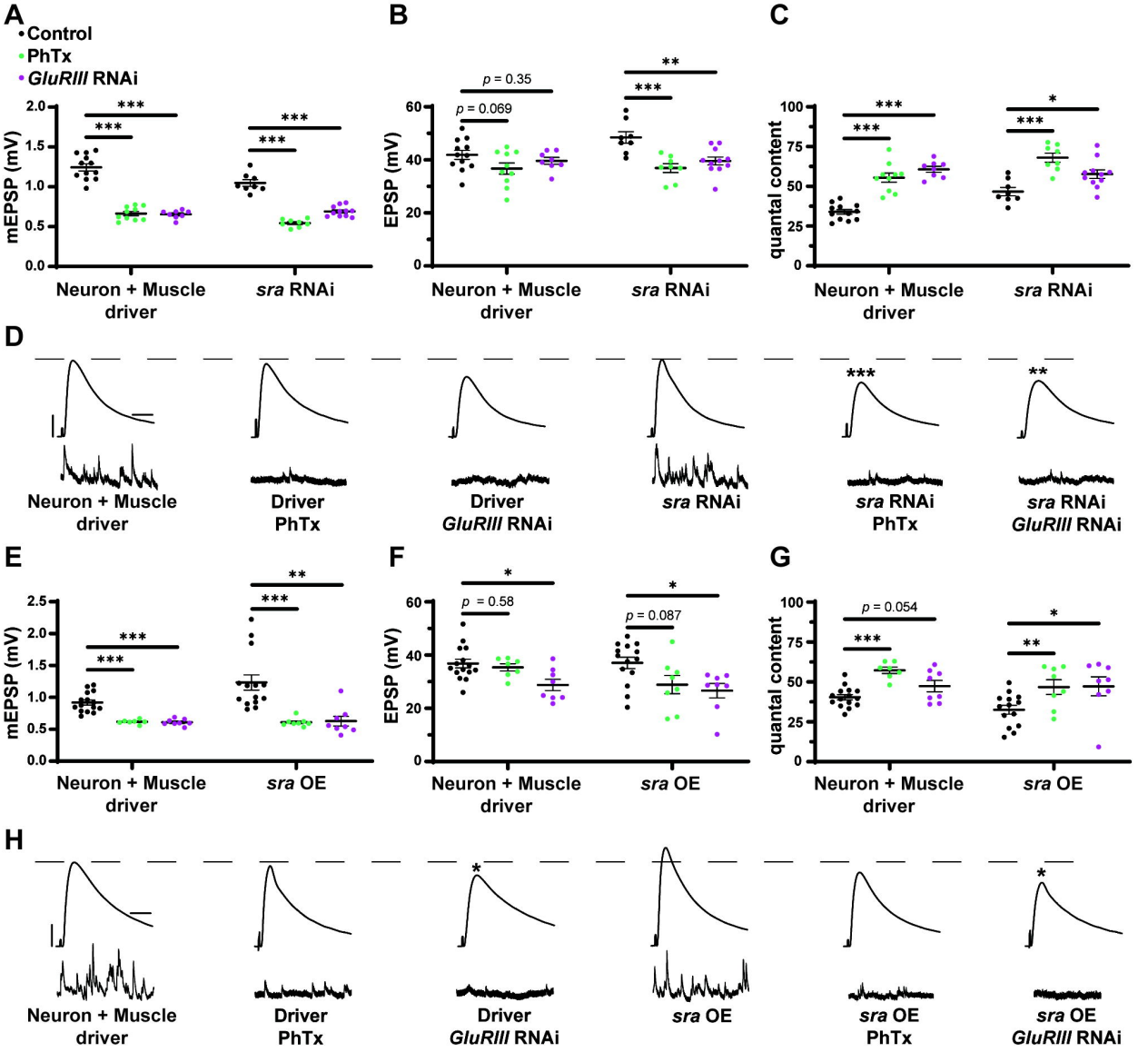
A
Control
PhTx
GluRIII RNAi
mEPSP (mV)
Neuron + Muscle driver
sra RNAi
B
EPSP (mV)
p = 0.35
p = 0.069
Neuron + Muscle driver
sra RNAi
C
quantal content
Neuron + Muscle driver
sra RNAi
D
Neuron + Muscle driver
Driver PhTx
Driver GluRIII RNAi
sra RNAi
sra RNAi PhTx
sra RNAi GluRIII RNAi
E
mEPSP (mV)
Neuron + Muscle driver
sra OE
F
EPSP (mV)
p = 0.58
p = 0.087
Neuron + Muscle driver
sra OE
G
quantal content
p = 0.054
Neuron + Muscle driver
sra OE
H
Neuron + Muscle driver
Driver PhTx
Driver GluRIII RNAi
sra OE
sra OE PhTx
sra OE GluRIII RNAi

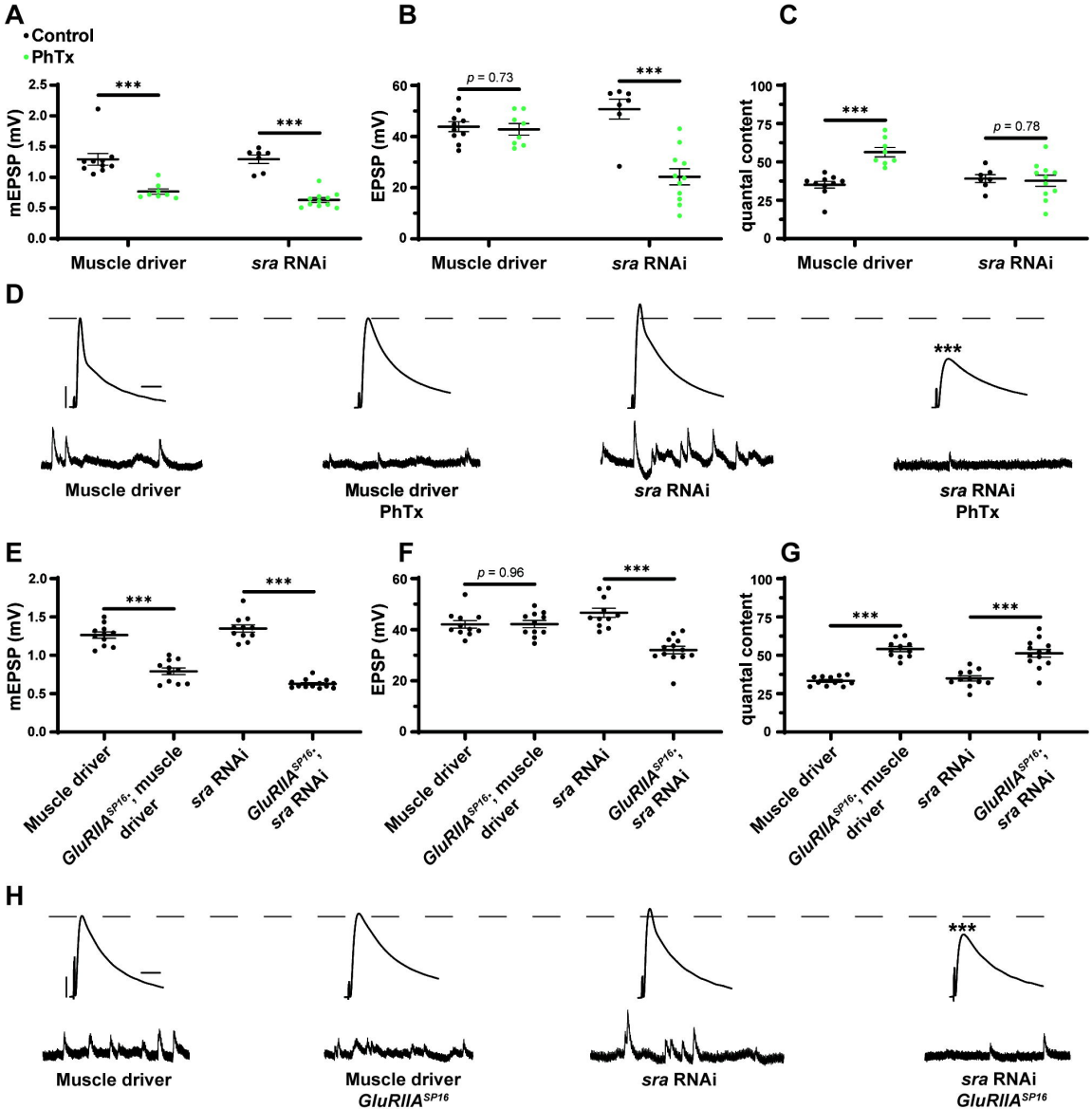
A
Control
PhTx
mEPSP (mV)
***
***
Muscle driver
sra RNAi
B
EPSP (mV)
p = 0.73
***
Muscle driver
sra RNAi
C
quantal content
***
p = 0.78
Muscle driver
sra RNAi
D
***
Muscle driver
Muscle driver PhTx
sra RNAi
sra RNAi PhTx
E
mEPSP (mV)
***
***
Muscle driver
GluRIIA^SP16/+; muscle driver
sra RNAi
GluRIIA^SP16/+; sra RNAi
F
EPSP (mV)
p = 0.96
***
Muscle driver
GluRIIA^SP16/+; muscle driver
sra RNAi
GluRIIA^SP16/+; sra RNAi
G
quantal content
***
***
Muscle driver
GluRIIA^SP16/+; muscle driver
sra RNAi
GluRIIA^SP16/+; sra RNAi
H
***
Muscle driver
Muscle driver GluRIIA^SP16
sra RNAi
sra RNAi GluRIIA^SP16

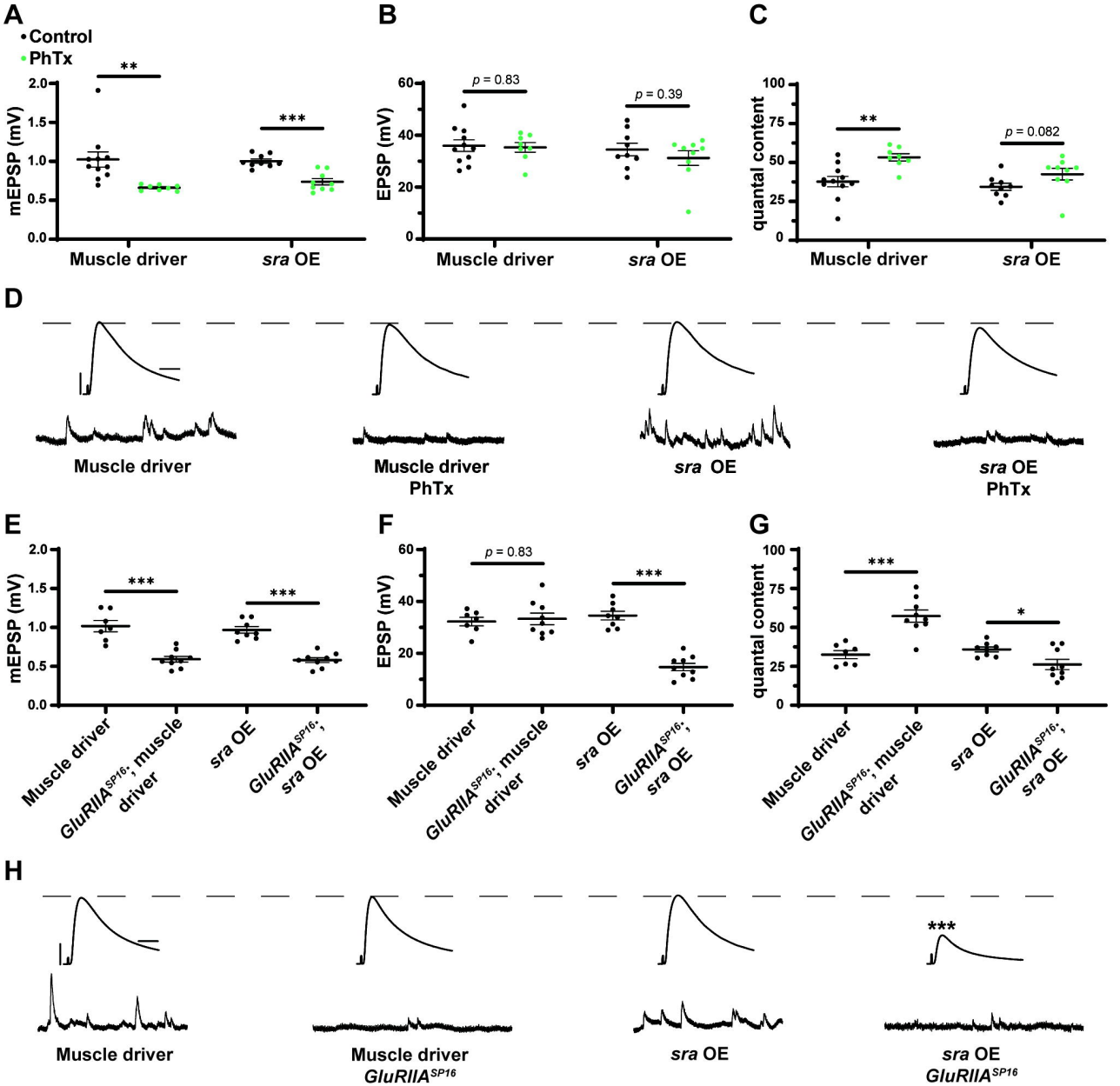
A
Control
PhTx
mEPSP (mV)
**
***
Muscle driver
sra OE
B
EPSP (mV)
p = 0.83
p = 0.39
Muscle driver
sra OE
C
quantal content
**
p = 0.082
Muscle driver
sra OE
D
Muscle driver
Muscle driver PhTx
sra OE
sra OE PhTx
E
mEPSP (mV)
***
***
Muscle driver
GluRIIA^SP16; muscle driver
sra OE
GluRIIA^SP16; sra OE
F
EPSP (mV)
p = 0.83
***
Muscle driver
GluRIIA^SP16; muscle driver
sra OE
GluRIIA^SP16; sra OE
G
quantal content
***
*
Muscle driver
GluRIIA^SP16; muscle driver
sra OE
GluRIIA^SP16; sra OE
H
***
Muscle driver
Muscle driver GluRIIA^SP16
sra OE
sra OE GluRIIA^SP16

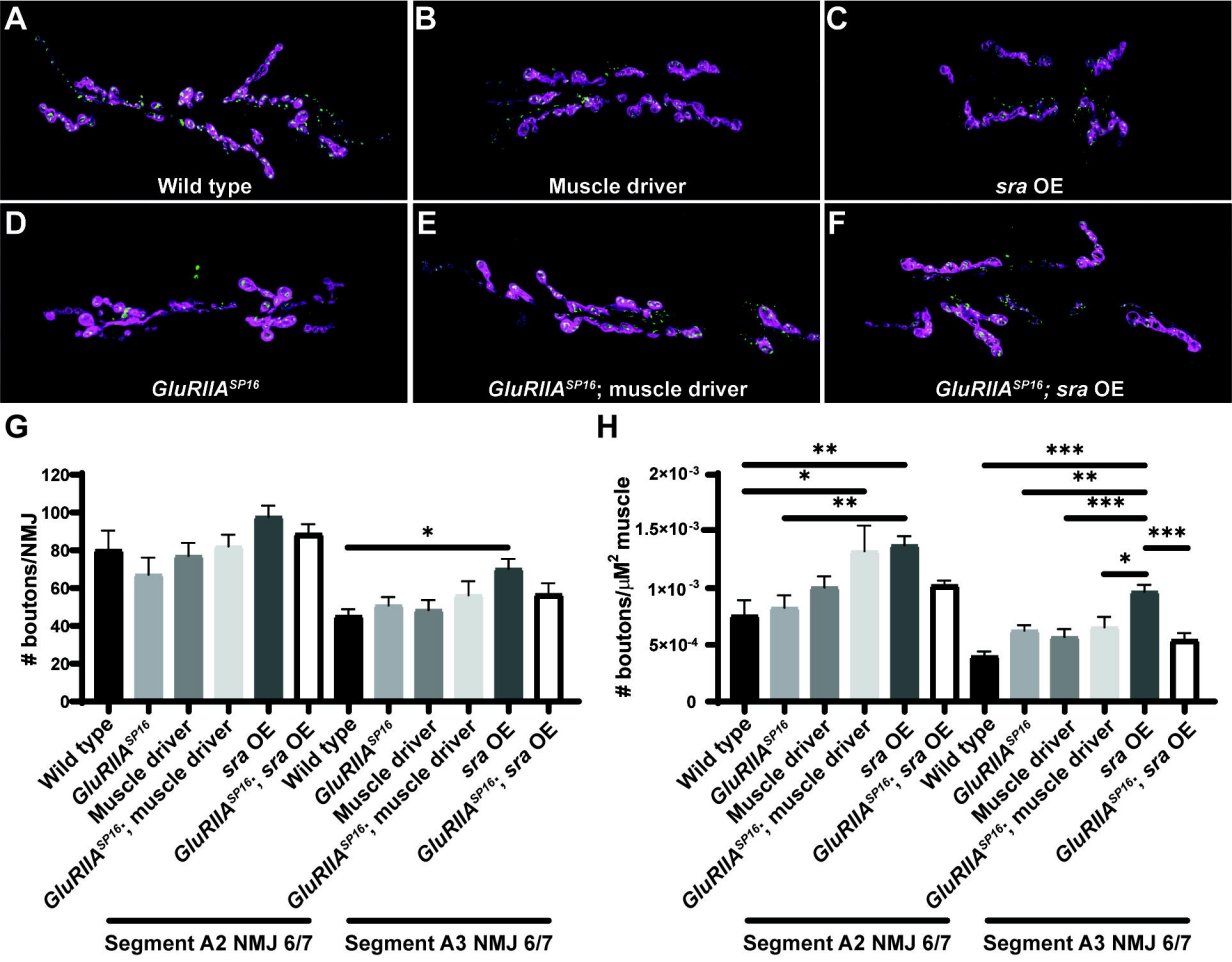
A
Wild type
B
Muscle driver
C
sra OE
D
GluRIIA^SP16
E
GluRIIA^SP16; muscle driver
F
GluRIIA^SP16; sra OE
G
boutons/NMJ
120
100
80
60
40
20
0
*
Wild type
GluRIIA^SP16
Muscle driver
GluRIIA^SP16; muscle driver
sra OE
GluRIIA^SP16; sra OE
Wild type
GluRIIA^SP16
Muscle driver
GluRIIA^SP16; muscle driver
sra OE
GluRIIA^SP16; sra OE
Segment A2 NMJ 6/7
Segment A3 NMJ 6/7
H
boutons/μM² muscle
2×10⁻³
1.5×10⁻³
1×10⁻³
5×10⁻⁴
0
**
*
**
***
**
***
*
***
Wild type
GluRIIA^SP16
Muscle driver
GluRIIA^SP16; muscle driver
sra OE
GluRIIA^SP16; sra OE
Wild type
GluRIIA^SP16
Muscle driver
GluRIIA^SP16; muscle driver
sra OE
GluRIIA^SP16; sra OE
Segment A2 NMJ 6/7
Segment A3 NMJ 6/7

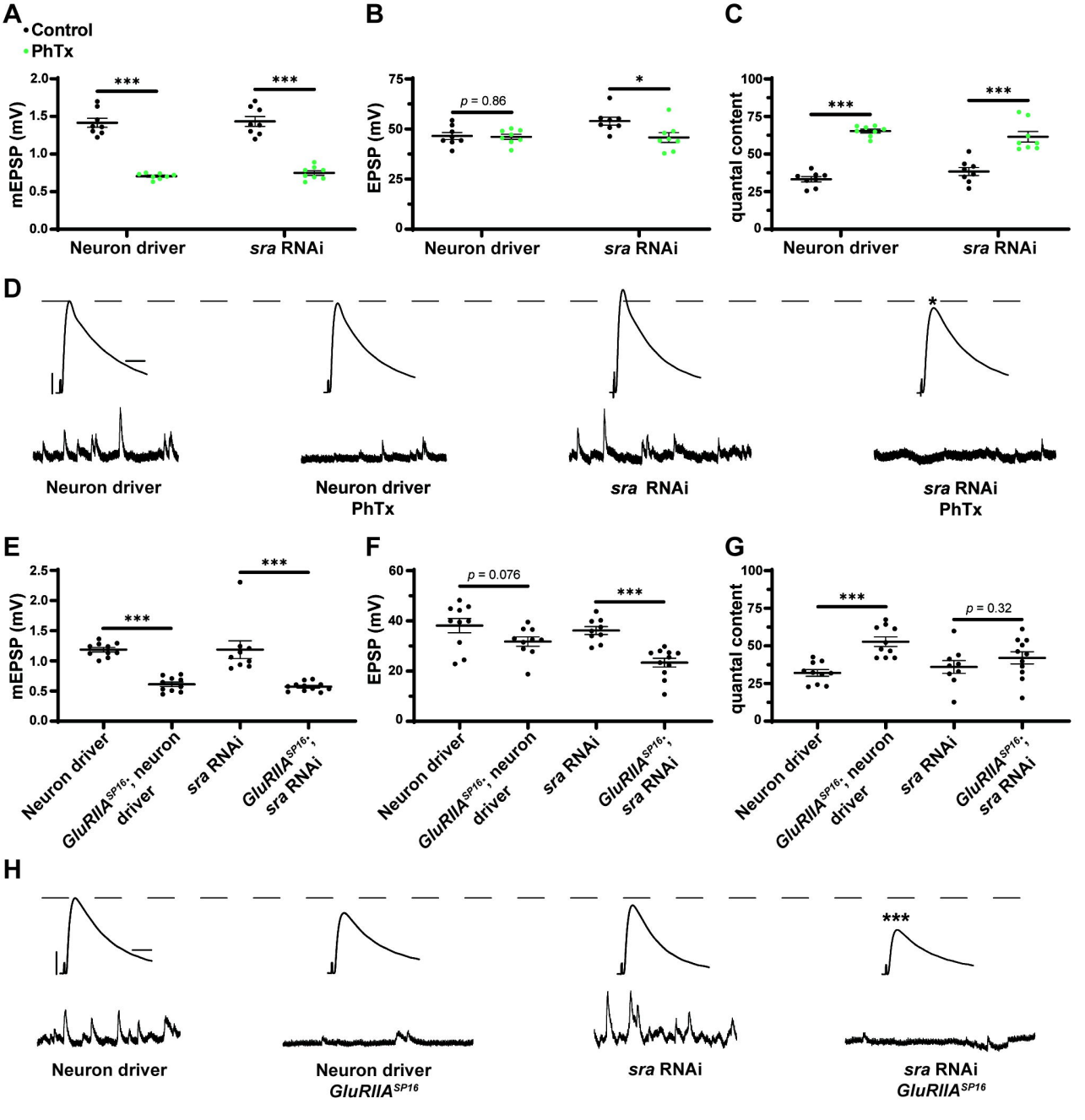
A
Control
PhTx
mEPSP (mV)
2.0
1.5
1.0
0.5
0.0
***
***
Neuron driver
sra RNAi
B
EPSP (mV)
75
50
25
0
p = 0.86
*
Neuron driver
sra RNAi
C
quantal content
100
75
50
25
0
***
***
Neuron driver
sra RNAi
D
*
Neuron driver
Neuron driver PhTx
sra RNAi
sra RNAi PhTx
E
mEPSP (mV)
2.5
2.0
1.5
1.0
0.5
0.0
***
***
Neuron driver
GluRIIA^SP16; neuron driver
sra RNAi
GluRIIA^SP16; sra RNAi
F
EPSP (mV)
60
40
20
0
p = 0.076
***
Neuron driver
GluRIIA^SP16; neuron driver
sra RNAi
GluRIIA^SP16; sra RNAi
G
quantal content
100
75
50
25
0
***
p = 0.32
Neuron driver
GluRIIA^SP16; neuron driver
sra RNAi
GluRIIA^SP16; sra RNAi
H
***
Neuron driver
Neuron driver GluRIIA^SP16
sra RNAi
sra RNAi GluRIIA^SP16

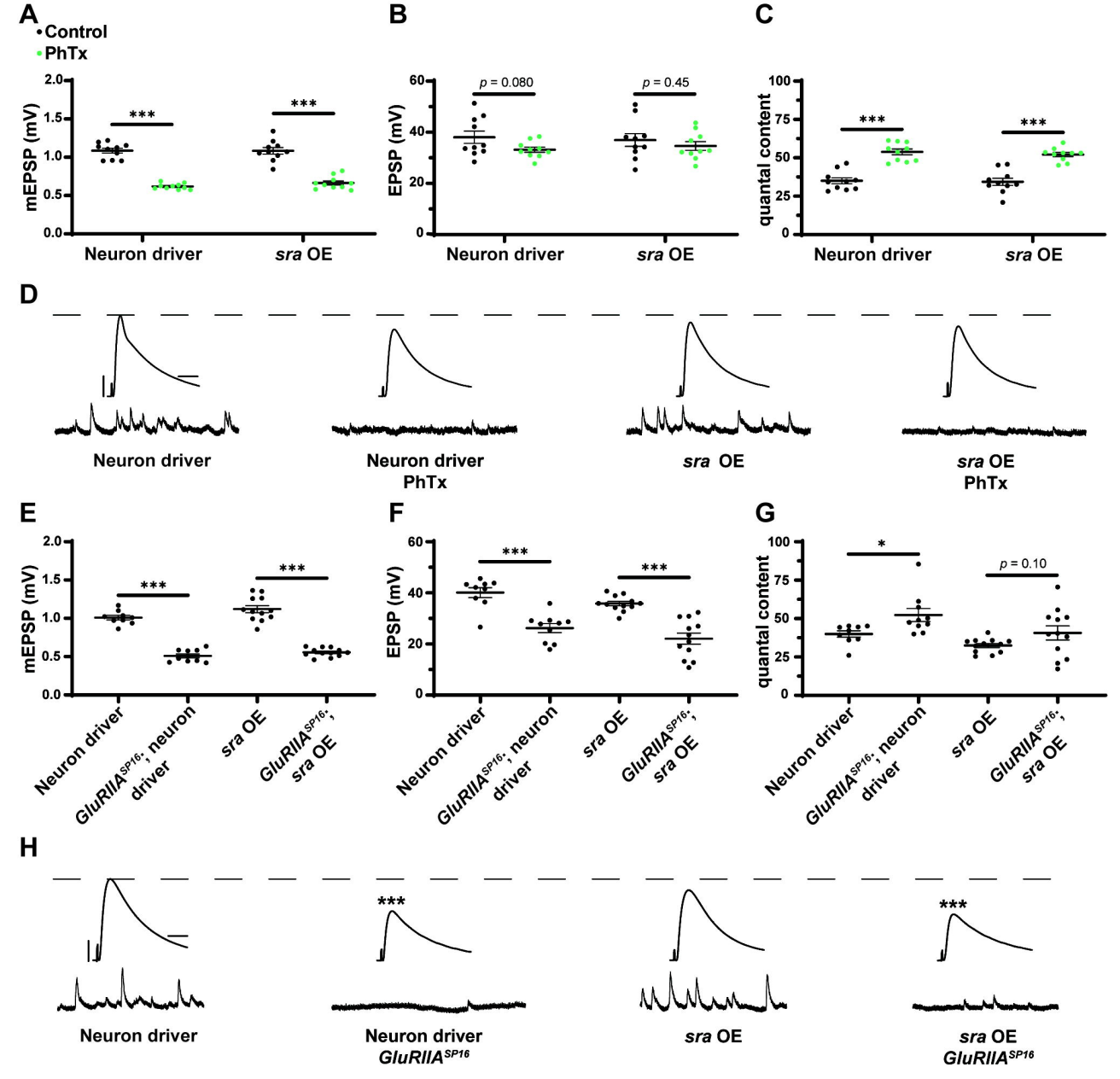
A
Control
PhTx
mEPSP (mV)
2.0
1.5
1.0
0.5
0.0
***
***
Neuron driver
sra OE
B
EPSP (mV)
60
40
20
0
p = 0.080
p = 0.45
Neuron driver
sra OE
C
quantal content
100
75
50
25
0
***
***
Neuron driver
sra OE
D
Neuron driver
Neuron driver PhTx
sra OE
sra OE PhTx
E
mEPSP (mV)
2.0
1.5
1.0
0.5
0.0
***
***
Neuron driver
GluRIIA SP16; neuron driver
sra OE
GluRIIA SP16; sra OE
F
EPSP (mV)
60
40
20
0
***
***
Neuron driver
GluRIIA SP16; neuron driver
sra OE
GluRIIA SP16; sra OE
G
quantal content
100
75
50
25
0
*
p = 0.10
Neuron driver
GluRIIA SP16; neuron driver
sra OE
GluRIIA SP16; sra OE
H
***
***
Neuron driver
Neuron driver GluRIIA SP16
sra OE
sra OE GluRIIA SP16

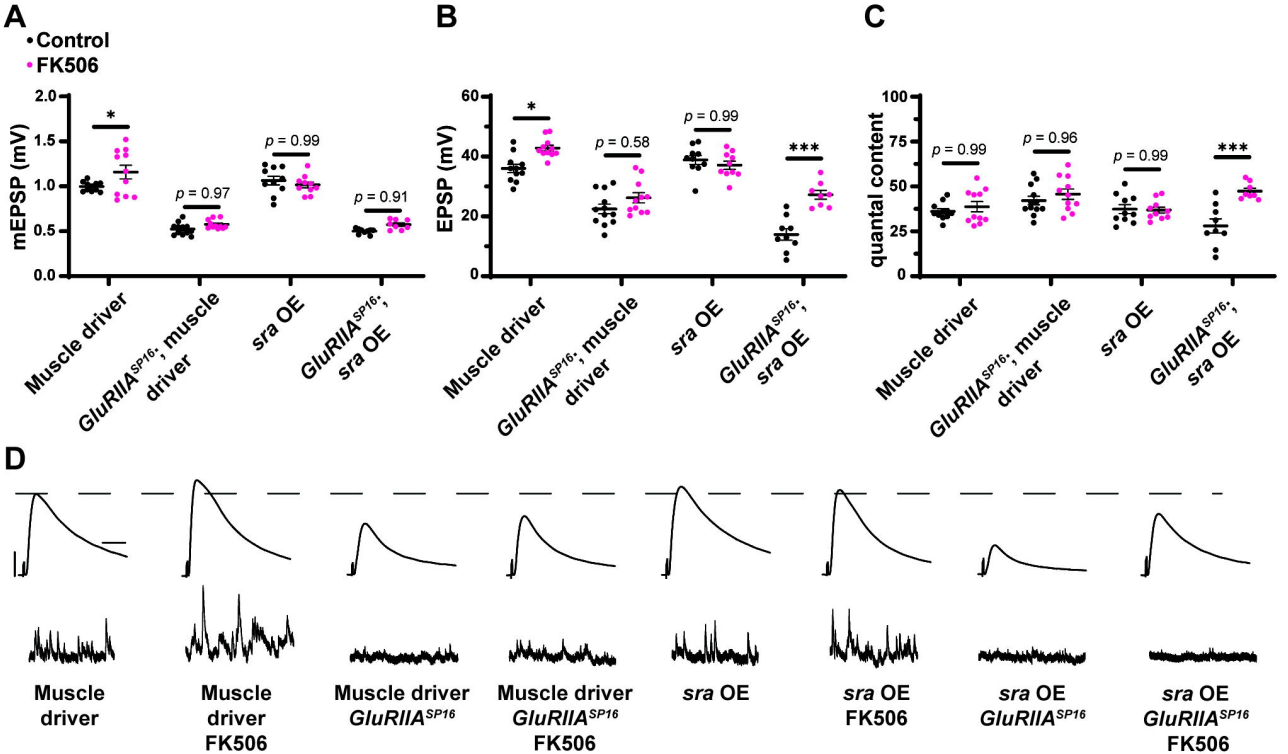
A
Control
FK506
mEPSP (mV)
2.0
1.5
1.0
0.5
0.0
*
p = 0.97
p = 0.99
p = 0.91
Muscle driver
GluRIIA^SP16; muscle driver
sra OE
GluRIIA^SP16; sra OE
B
EPSP (mV)
60
40
20
0
*
p = 0.58
p = 0.99
***
Muscle driver
GluRIIA^SP16; muscle driver
sra OE
GluRIIA^SP16; sra OE
C
quantal content
100
75
50
25
0
p = 0.99
p = 0.96
p = 0.99
***
Muscle driver
GluRIIA^SP16; muscle driver
sra OE
GluRIIA^SP16; sra OE
D
Muscle driver
Muscle driver FK506
Muscle driver GluRIIA^SP16
Muscle driver GluRIIA^SP16 FK506
sra OE
sra OE FK506
sra OE GluRIIA^SP16
sra OE GluRIIA^SP16 FK506

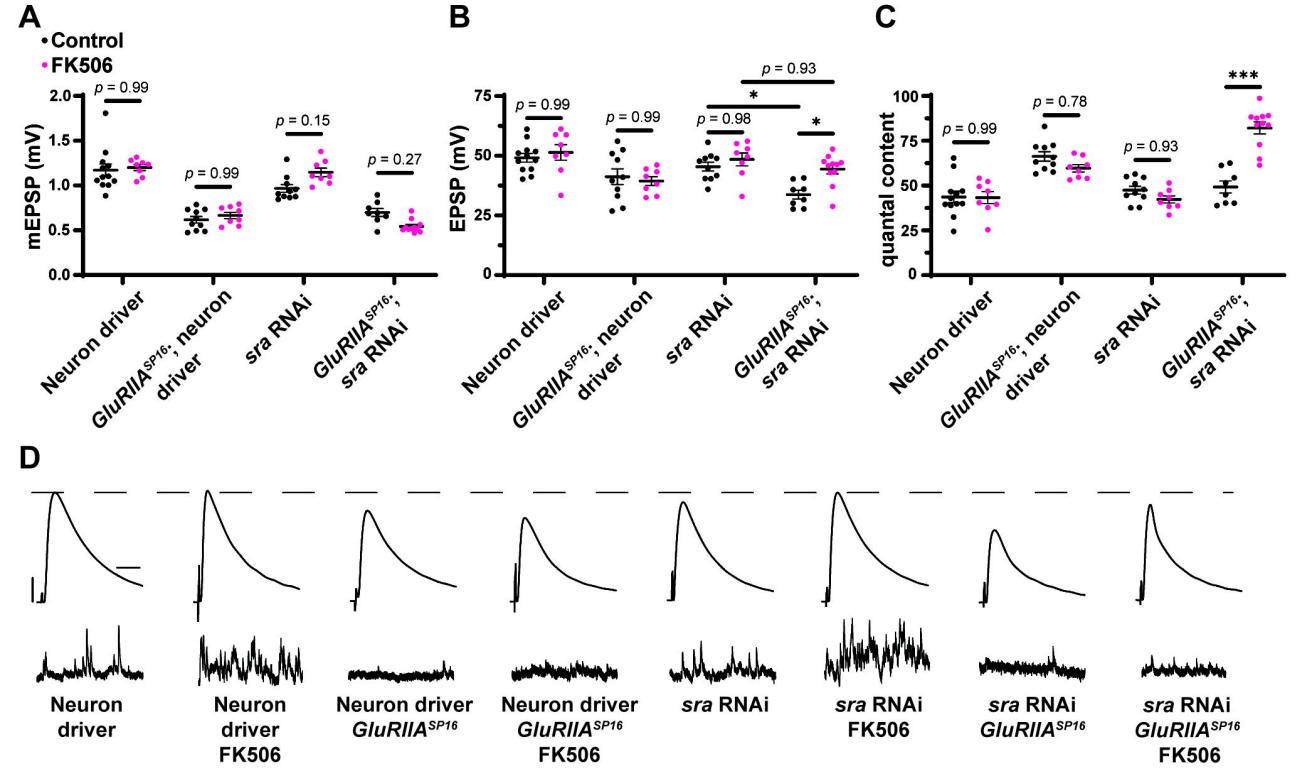
A
Control
FK506
mEPSP (mV)
2.0
1.5
1.0
0.5
0.0
p = 0.99
p = 0.99
p = 0.15
p = 0.27
Neuron driver
GluRIIA^SP16; neuron driver
sra RNAi
GluRIIA^SP16; sra RNAi
B
EPSP (mV)
75
50
25
0
p = 0.99
p = 0.99
p = 0.98
p = 0.93
*
*
Neuron driver
GluRIIA^SP16; neuron driver
sra RNAi
GluRIIA^SP16; sra RNAi
C
quantal content
100
75
50
25
0
p = 0.99
p = 0.78
p = 0.93
***
Neuron driver
GluRIIA^SP16; neuron driver
sra RNAi
GluRIIA^SP16; sra RNAi
D
Neuron driver
Neuron driver FK506
Neuron driver GluRIIA^SP16
Neuron driver GluRIIA^SP16 FK506
sra RNAi
sra RNAi FK506
sra RNAi GluRIIA^SP16
sra RNAi GluRIIA^SP16 FK506

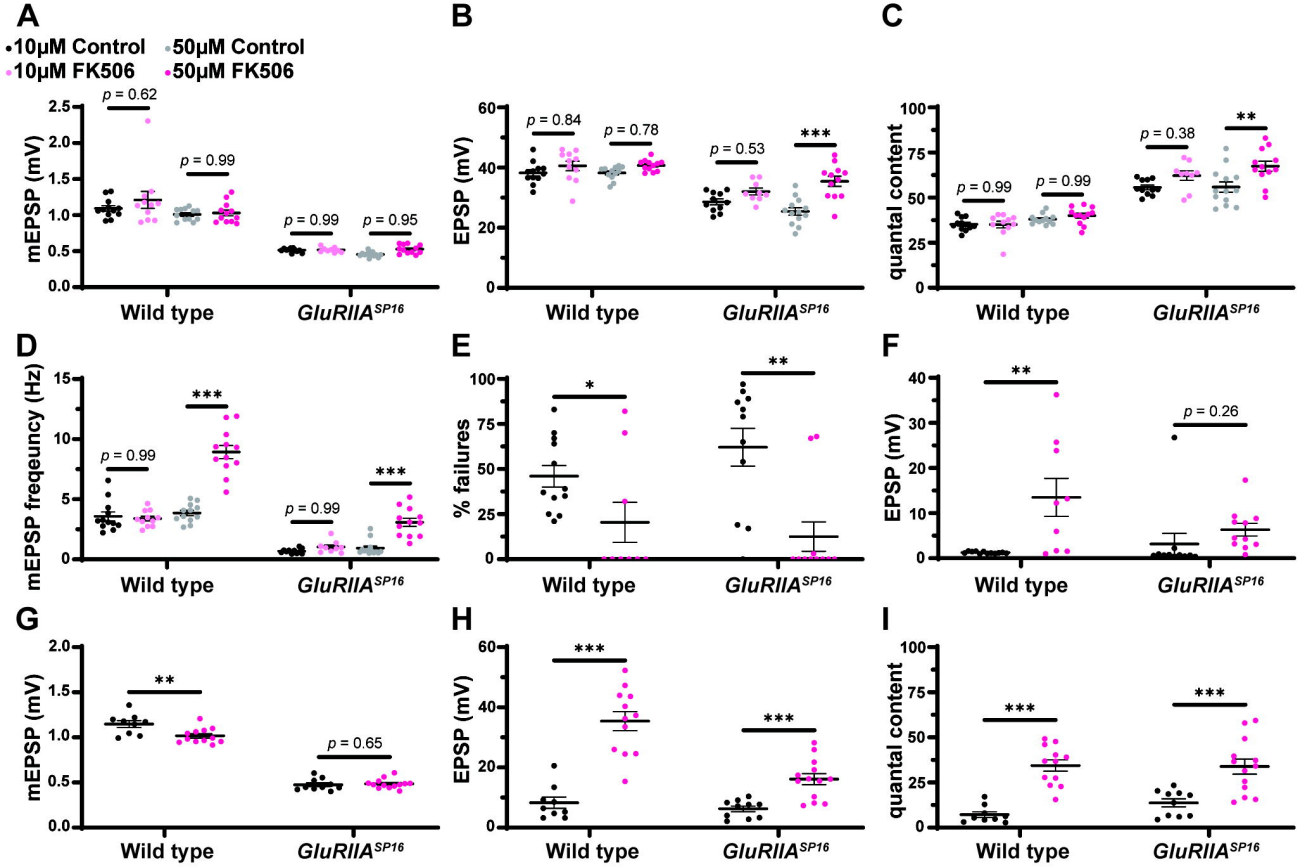
A
B
C
D
E
F
G
H
I
10μM Control
50μM Control
10μM FK506
50μM FK506
mEPSP (mV)
EPSP (mV)
quantal content
mEPSP freqeuncy (Hz)
% failures
p = 0.62
p = 0.99
p = 0.99
p = 0.95
p = 0.84
p = 0.78
p = 0.53
***
p = 0.99
p = 0.38
**
p = 0.99
***
p = 0.99
***
*
**
**
p = 0.26
**
p = 0.65
***
***
***
***
Wild type
GluRIIA^SP16